Elettra: Science Highlights and Machine Developments

G. Paolucci
Chief Scientific Officer
Elettra-Sincrotrone Trieste

Elettra-Sincrotrone Trieste S.C.p.A.

A nonprofit shareholder company "of national interest":

AREA Science Park	53.7%
FVG Regional Government	37.6%
CNR	4.9%
Invitalia Partecipazioni S.p.A.	3.8%

- Established in 1987 to construct and manage synchrotron light sources – international facility
- Promote cultural and socioeconomic growth at the regional, national and international level
- State-of-the art research facilities, technical leadership, skill development and transfer

PAYROLL: 395 STAFF + 102 POSTDOCS/TRAINEES

TURNOVER: 56 M€/Yr

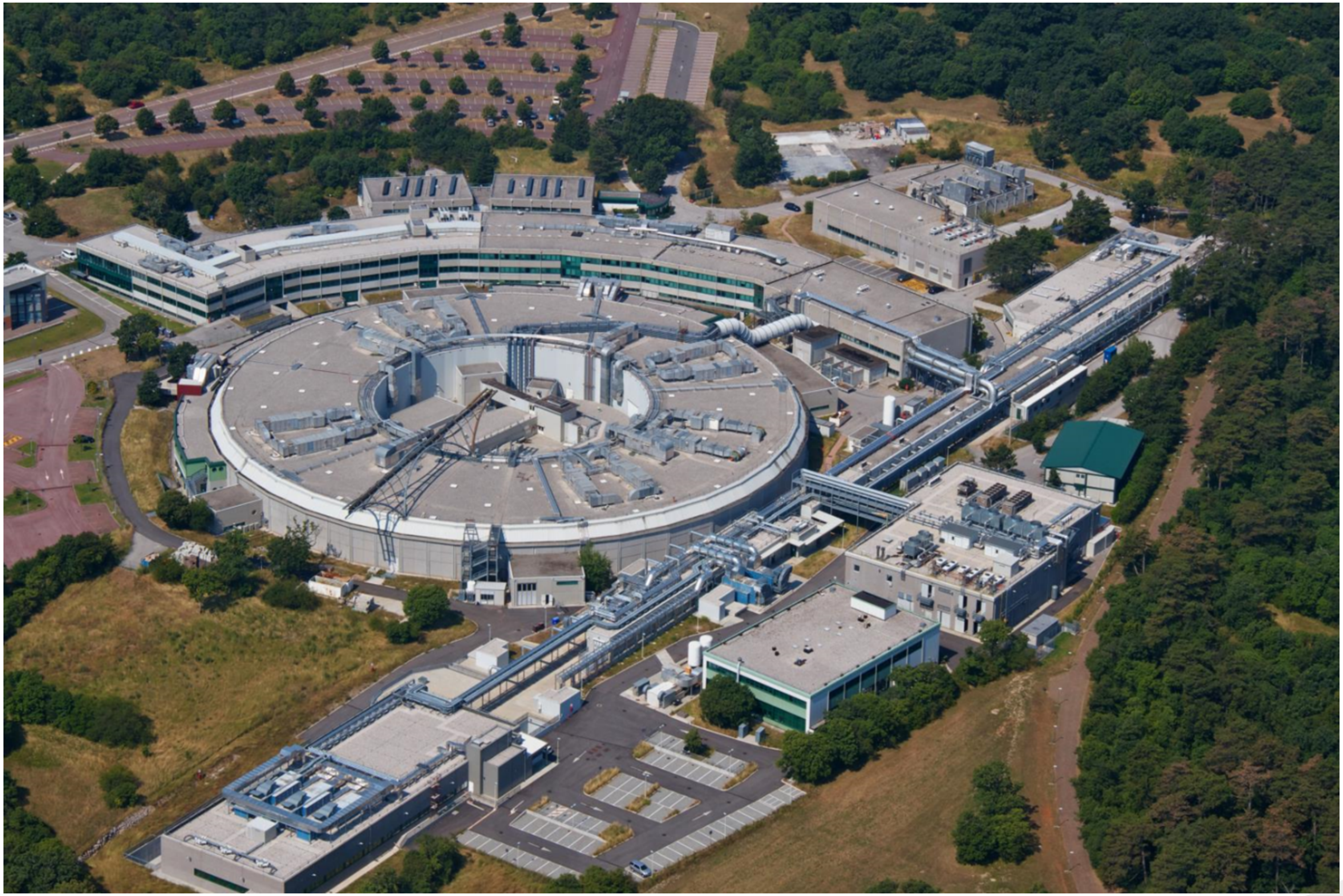

Elettra
Sincrotrone
Trieste

Elettra 2.0-2.4 GeV 3rd generation Synchrotron Radiation Facility

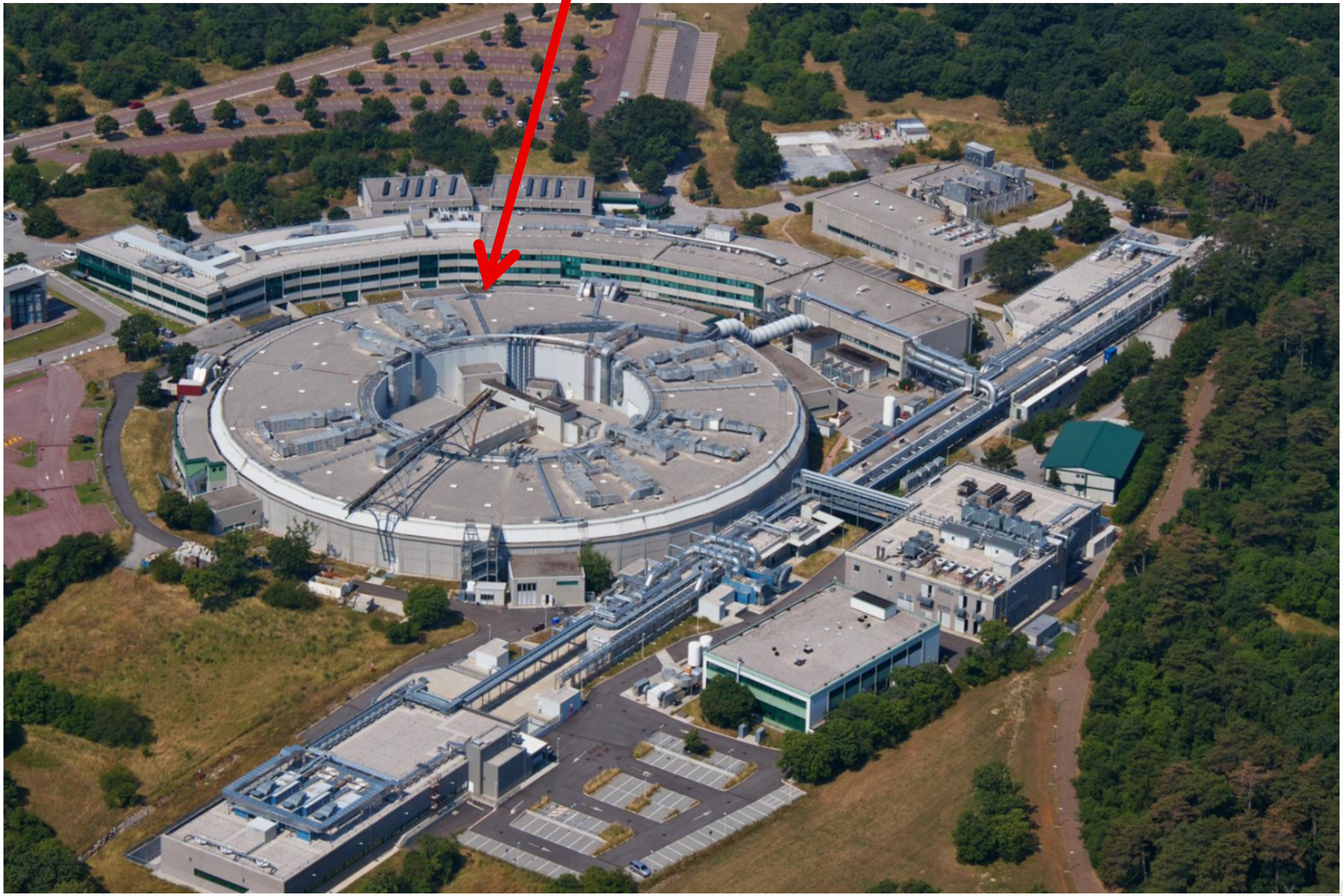

Elettra
Sincrotrone
Trieste

Elettra 2.0-2.4 GeV 3rd generation Synchrotron Radiation Facility

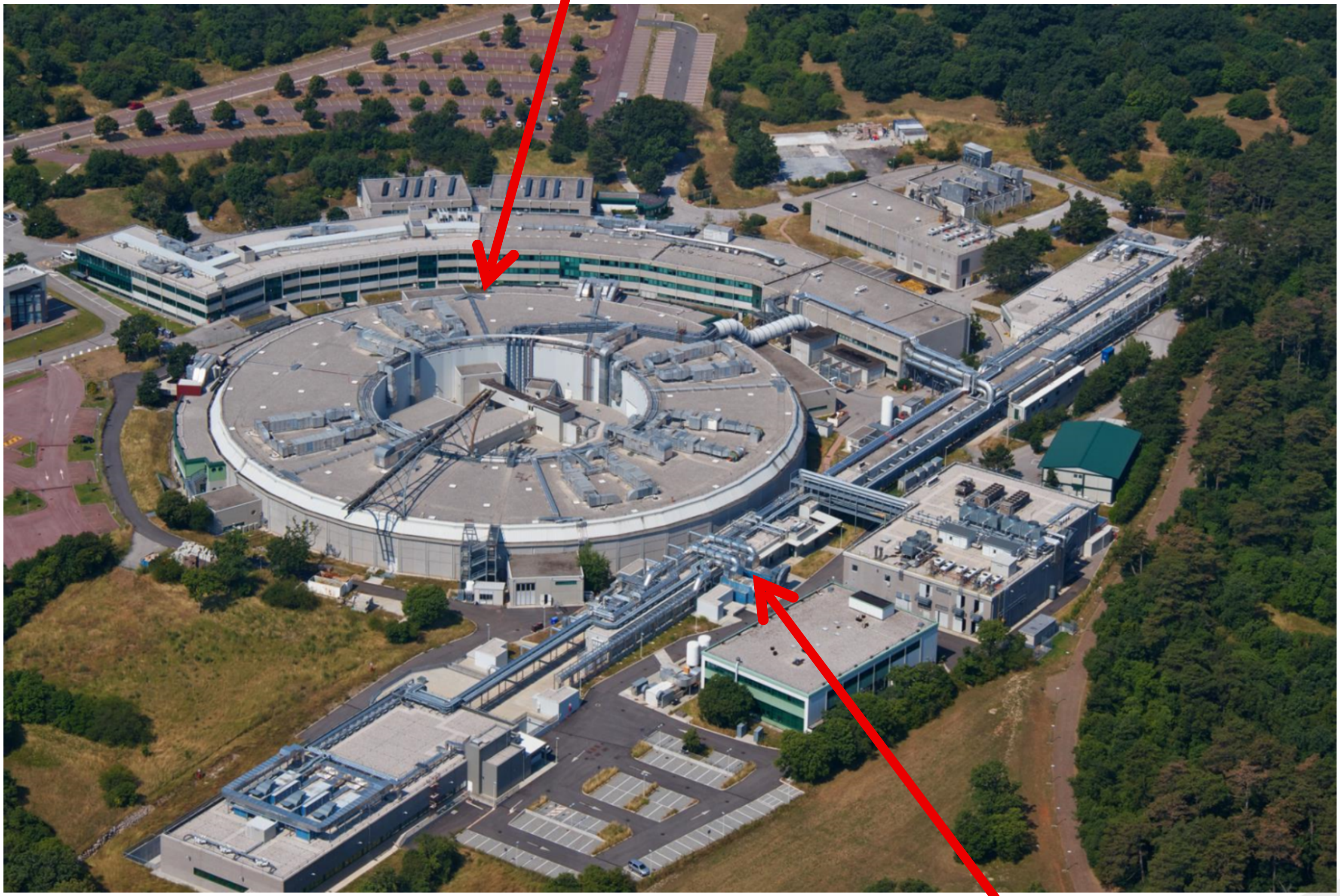

FERMI 1.5 GeV seeded Free Electron Laser Facility

Elettra
Sincrotrone
Trieste

Elettra 2.0-2.4 GeV 3rd generation Synchrotron Radiation Facility

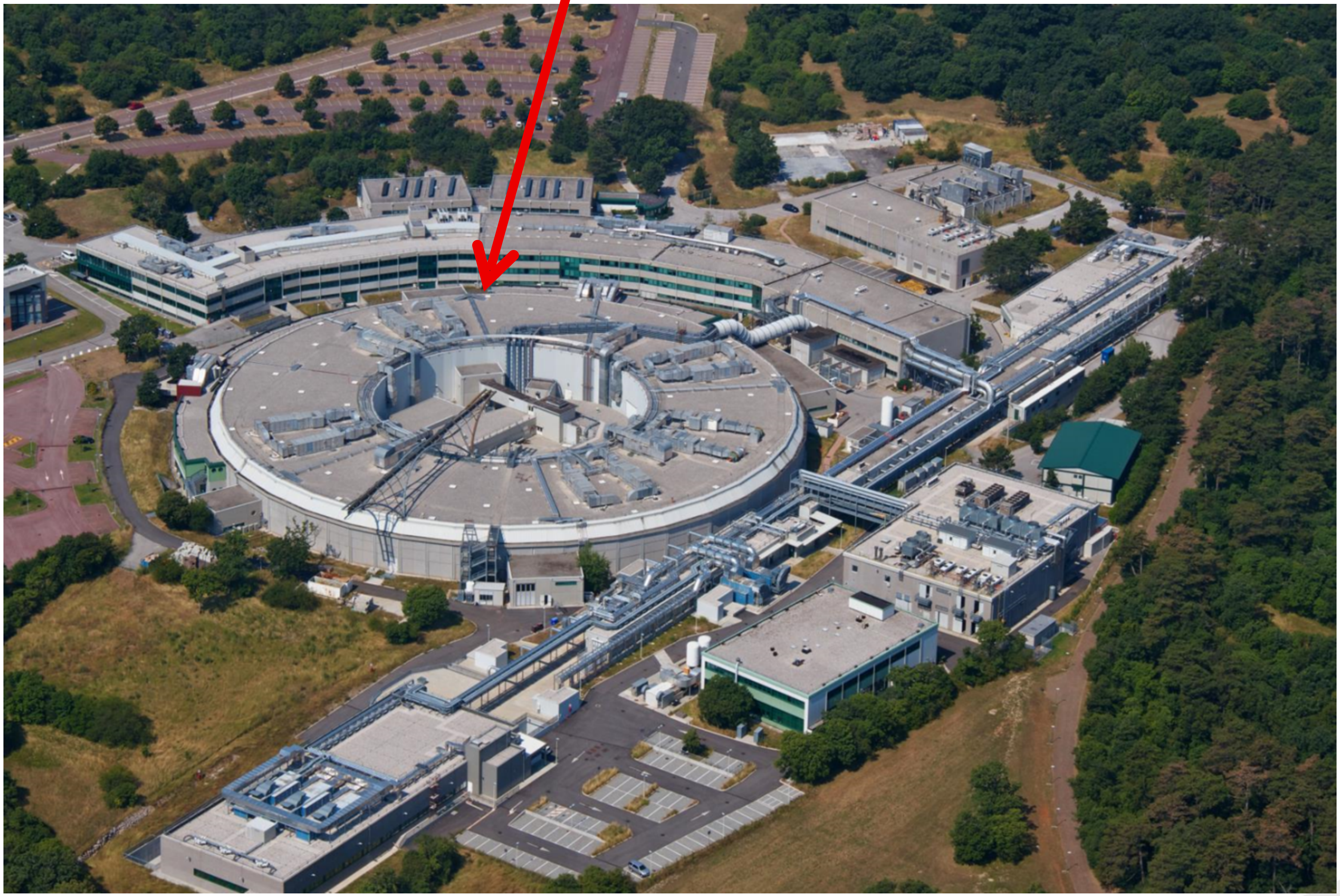

CERTIFIED MANAGEMENT SYSTEM
CQY CERTIQUALITY
UNI EN ISO 9001:2015
UNI ISO 45001:2018

Elettra: national and international partnerships

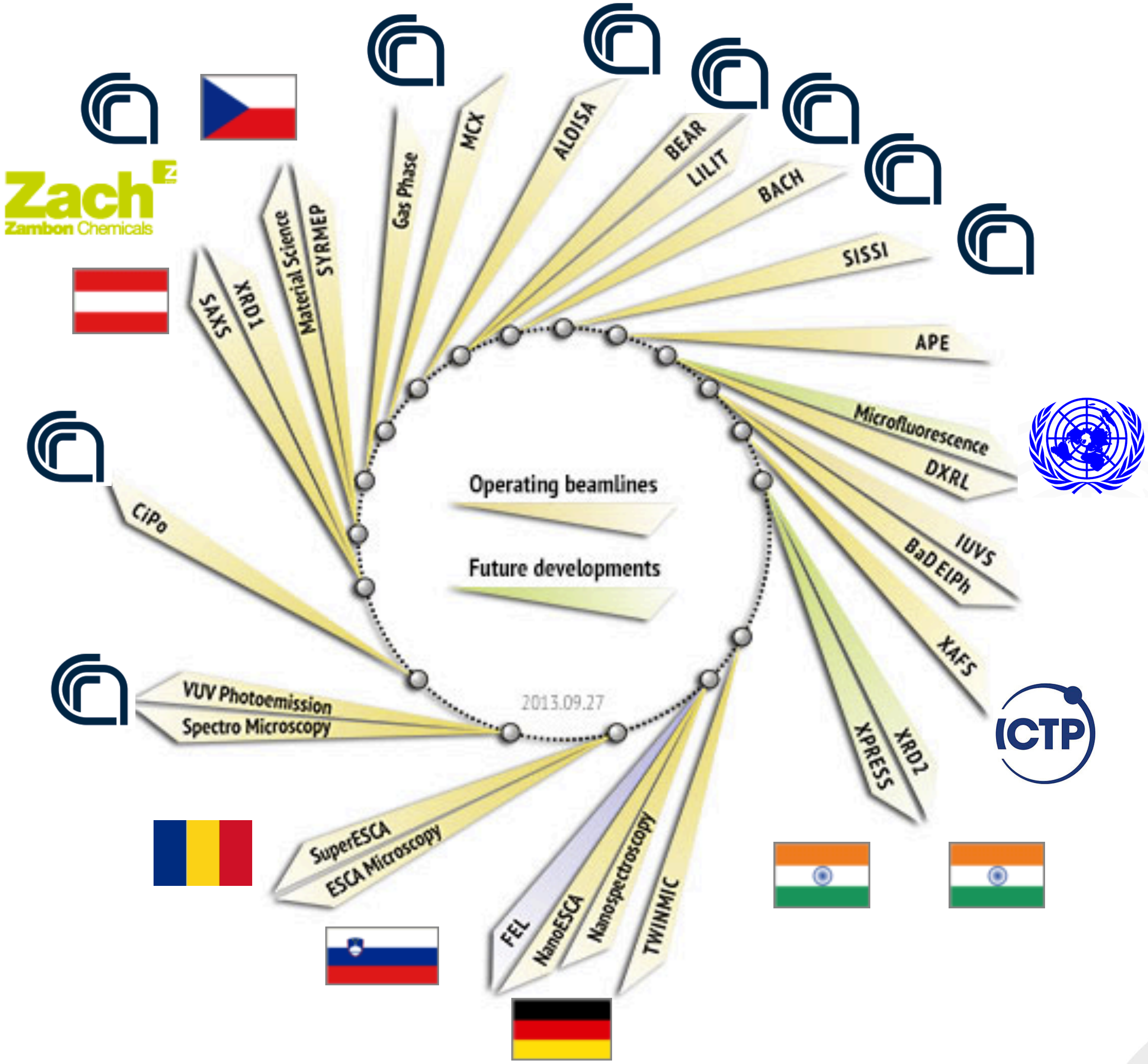

Over 1100 experiments proposed in 2021…

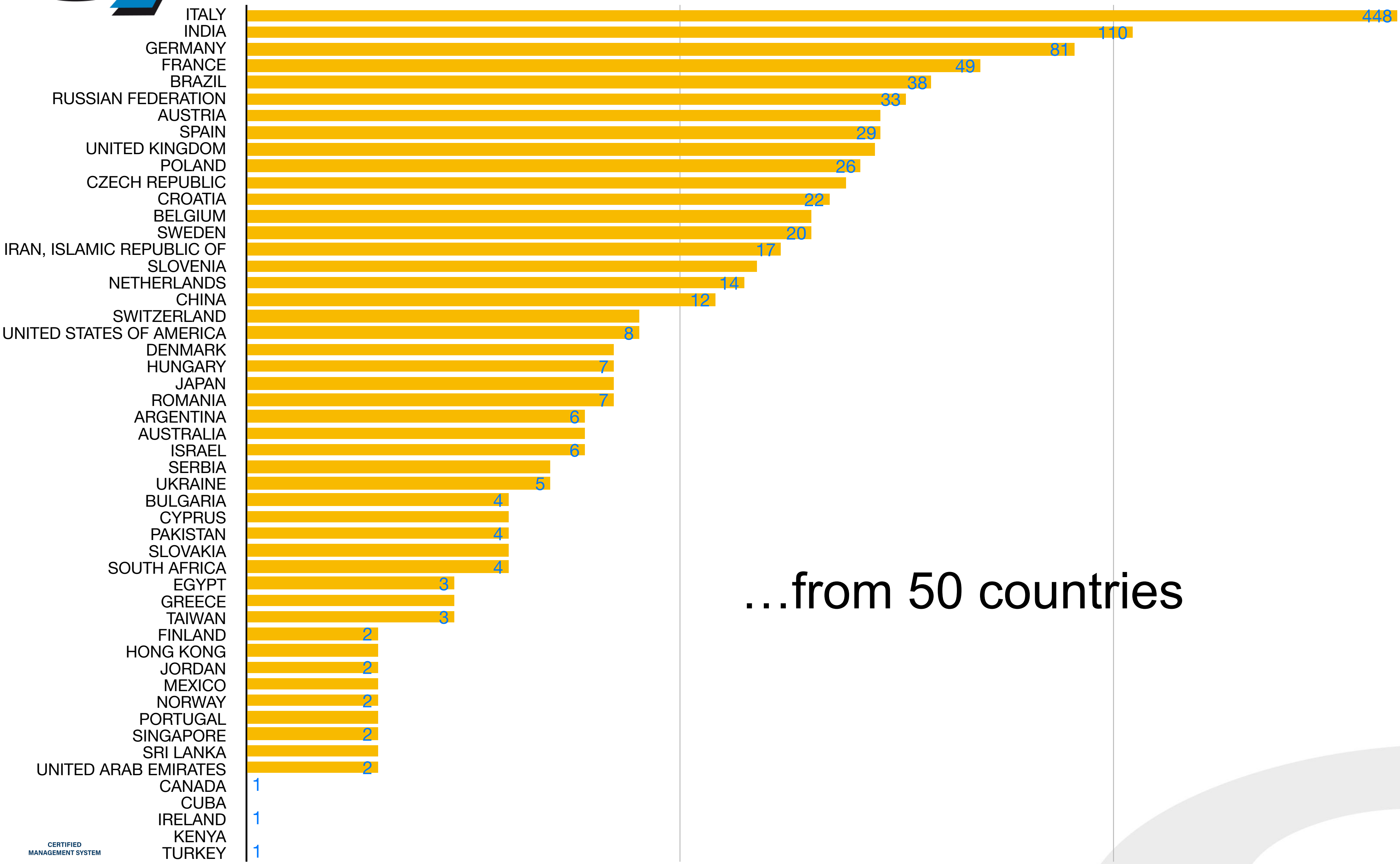

…from 50 countries

Elettra Sincrotrone Trieste

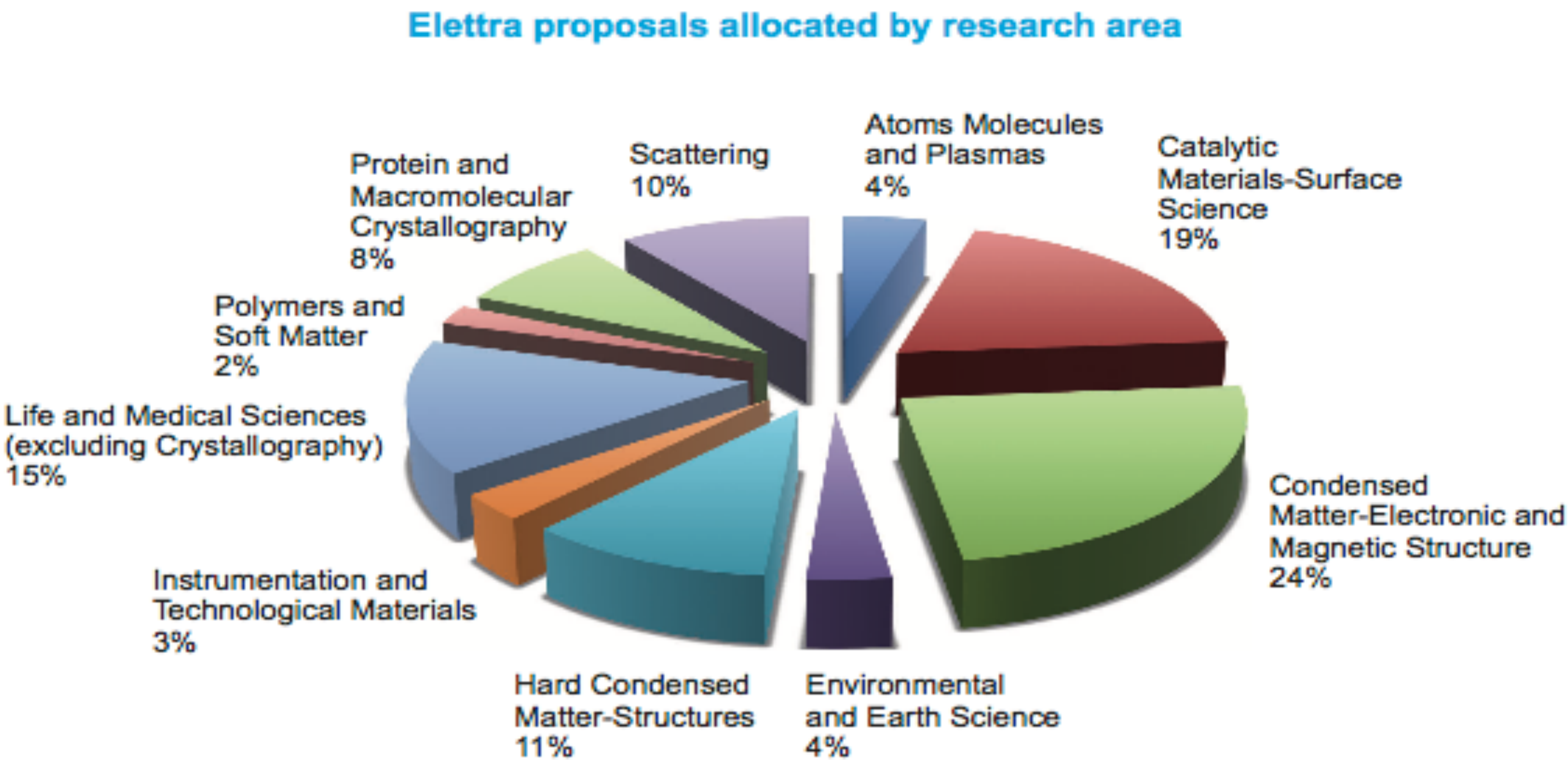

Novel materials, novel characterization and processing techniques, nano- and life sciences

>1200 proposals in 2017

from > 50 countries

438 ISI publications

CERTIFIED MANAGEMENT SYSTEM CQY CERTIQUALITY UNI EN ISO 9001:2015 UNI ISO 45001:2018

Publications from the Elettra SR and labs in 2022 (2021)

552 (540) Articles on peer reviewed journals

17 (15) Conference proceedings

1 (5) Books/chapters

Elettra
Sincrotrone
Trieste

Photoelectron spectroscopy

SuperESCA

Elettra Sincrotrone Trieste

ACS APPLIED MATERIALS & INTERFACES

www.acsami.org

Research Article

Probing the Atomic Arrangement of Subsurface Dopants in a Silicon Quantum Device Platform

Håkon I. Røst, Ezequiel Tosi, Frode S. Strand, Anna Cecilie Åsland, Paolo Lacovig, Silvano Lizzit, and Justin W. Wells*

Cite This: *ACS Appl. Mater. Interfaces* 2023, 15, 22637–22643

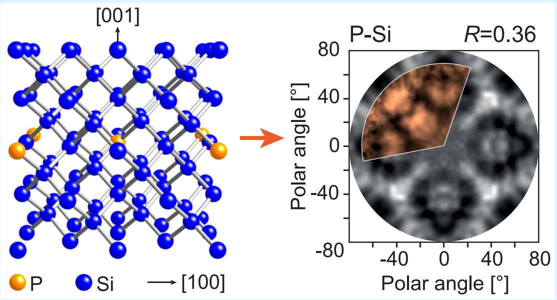

ABSTRACT: High-density structures of subsurface phosphorus dopants in silicon continue to garner interest as a silicon-based quantum computer platform; however, a much-needed confirmation of their dopant arrangement has been lacking. In this work, we take advantage of the chemical specificity of X-ray photoelectron diffraction to obtain the precise structural configuration of P dopants in subsurface Si:P δ-layers. The growth of δ-layer systems with different levels of doping is carefully studied and verified using X-ray photoelectron spectroscopy and low-energy electron diffraction. Subsequent diffraction measurements reveal that in all cases, the subsurface dopants primarily substitute with Si atoms from the host material. Furthermore, no signs of carrier-inhibiting P−P dimerization can be observed. Our observations not only settle a nearly decade-long debate about the dopant arrangement but also demonstrate how X-ray photoelectron diffraction is surprisingly well suited for studying subsurface dopant structure. This work thus provides valuable input for an updated understanding of the behavior of Si:P δ-layers and the modeling of their derived quantum devices.

KEYWORDS: *delta-layers, quantum electronic devices, quantum computing, photoemission, photoelectron diffraction*

SuperESCA (ACS Appl. Mater. Interfaces 2023, 15, 22637−22643)

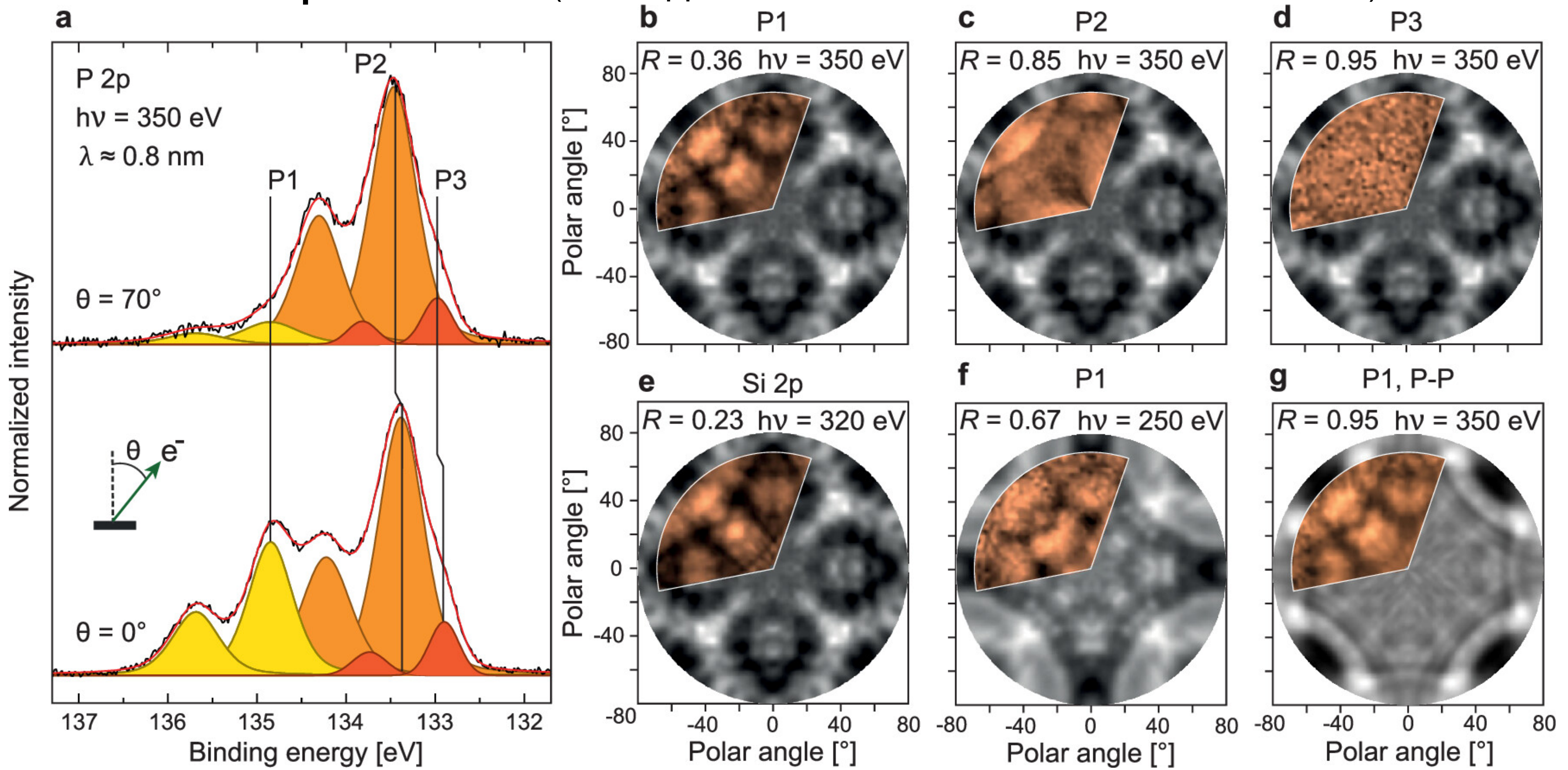

Angle-dependent photoelectron spectroscopy from a “double-dosed”, Si-encapsulated δ-layer. (a) XPS of the P 2p peak, measured with hν = 350 eV at normal (θ = 0°) and grazing (θ = 70°) emission and an integrated half-angle acceptance of ≤5°. P1 comes from P in the δ-layer, and P2 and P3 from P near the Si surface. Both spectra have been scaled to the intensity of P2. (b–d) The measured (orange) and calculated (gray) XPD patterns for the peaks P1–P3 from the double-dosed δ-layer system shown in (a). (e) The measured and calculated XPD from the corresponding Si 2p core level. (f) The measured XPD from P1 at hν = 250 eV, compared with XPD simulations of P–Si bonding (i.e., substitutional doping) within the δ-layer. (g) The measured XPD of P1 at hν = 350 eV from (b), compared with XPD simulations of P–P bonding (i.e., dimerization) within the δ-layer.

Elettra
Sincrotrone
Trieste

Photoelectron microscopy

ESCAmicroscopy

Applied Surface Science 610 (2023) 155497

Contents lists available at ScienceDirect

Applied Surface Science

journal homepage: www.elsevier.com/locate/apsusc

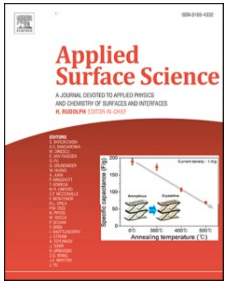

Full Length Article

Understanding carbide evolution and surface chemistry during deep cryogenic treatment in high-alloyed ferrous alloy

Patricia Jovičević-Klug [a,b,*], Levi Tegg [c,d], Matic Jovičević-Klug [b], Rahul Parmar [e], Matteo Amati [e], Luca Gregoratti [e], László Almásy [f], Julie M. Cairney [c,d], Bojan Podgornik [a]

[a] *Institute of Metals and Technology, Lepi pot 11, 1000 Ljubljana, Slovenia*
[b] *Max-Planck Institute for Iron Research, Max-Planck-Str. 1, 40237 Düsseldorf, Germany*
[c] *School of Aerospace, Mechanical and Mechatronic Engineering, The University of Sydney, Camperdown, NSW 2006, Australia*
[d] *Australian Centre for Microscopy and Microanalysis, The University of Sydney, Camperdown, NSW 2006, Australia*
[e] *Elettra - Sincrotone Trieste, S.C.p.A., SS14 – km 163.5 in Area Science Park, 34149 Trieste, Italy*
[f] *Institute for Energy Security and Environmental Safety, Centre for Energy Research, Konkoly-Thege Miklos út. 29-33, 1121 Budapest, Hungary*

ESCAmicroscopy (Applied Surface Science 610 (2023) 155497)

Elettra Sincrotrone Trieste

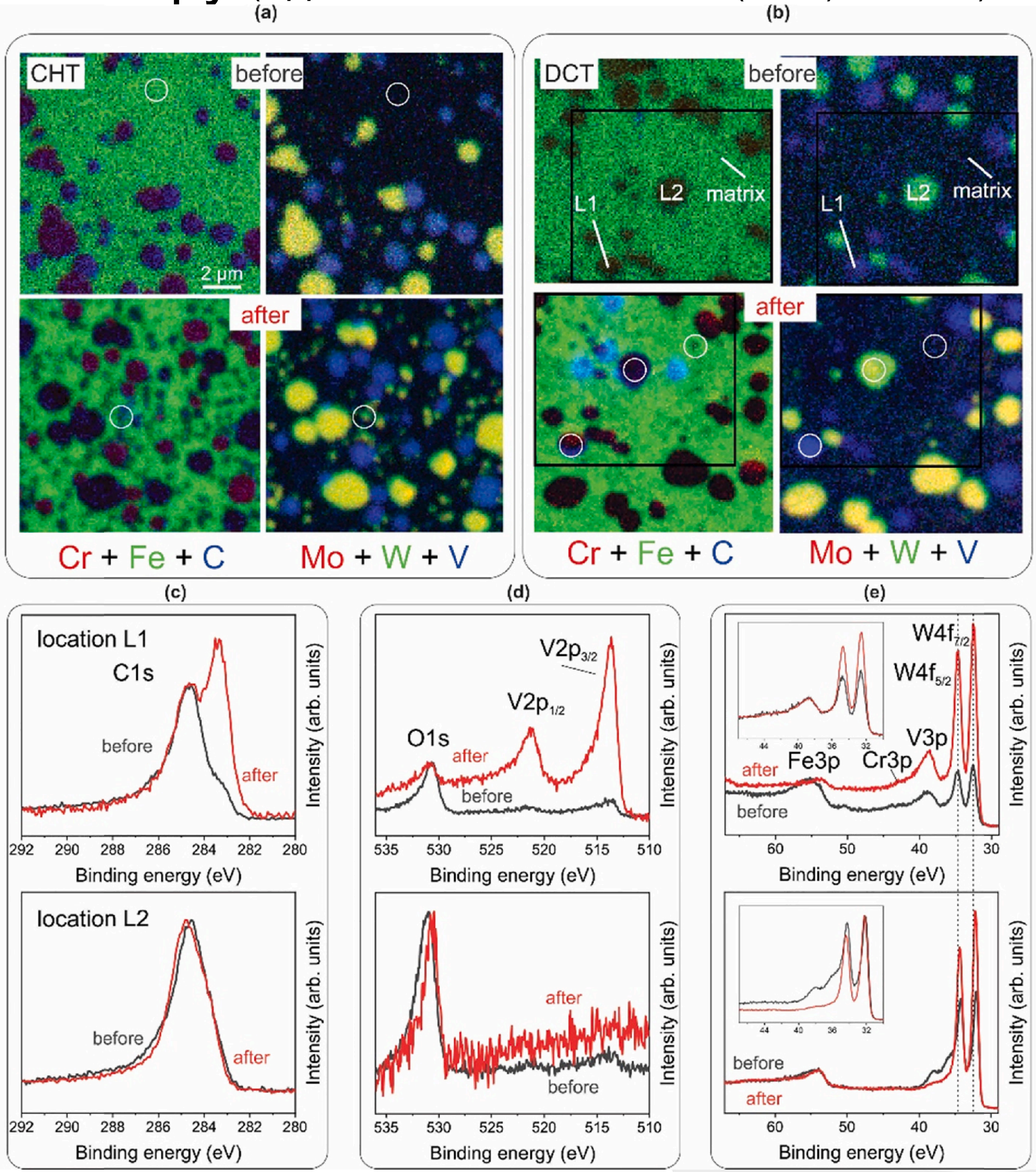

SPEM color-coded elemental maps of selected areas of (a) the CHT and (b) the DCT sample before (top) and after (bottom) tempering. The white circles indicate the exemplar positions probed for point-analysis with XPS. (c)-(e) XPS chemical spectra of the larger MC (top) and M6C (bottom) carbides before (dark color) and after (red color) tempering, for (c) C1s (d) V2p and (e) Fe3p, Cr3p, V3p and W4f. The data represents the chemical state of both carbide types for both CHT and DCT samples.

Elettra
Sincrotrone
Trieste

Cultural heritage

Elettra
Sincrotrone
Trieste

SISSI-Bio

analytical chemistry

pubs.acs.org/ac Letter

A Nanofocused Light on Stradivari Violins: Infrared s-SNOM Reveals New Clues Behind Craftsmanship Mastery

Chiaramaria Stani, Claudia Invernizzi, Giovanni Birarda, Patrizia Davit, Lisa Vaccari,* Marco Malagodi,* Monica Gulmini, and Giacomo Fiocco

Cite This: *Anal. Chem.* 2022, 94, 14815–14819 Read Online

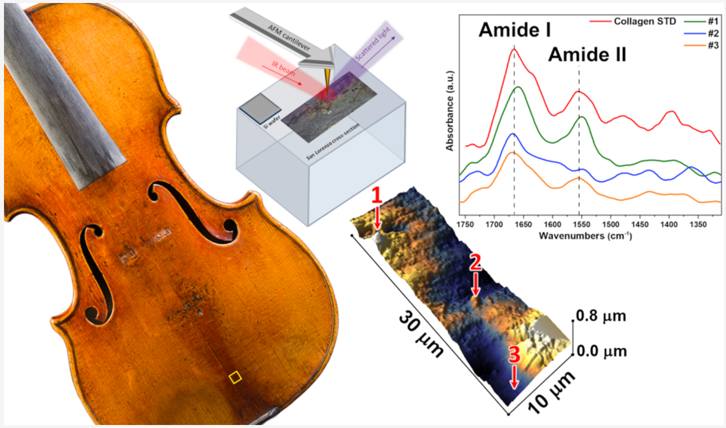

ABSTRACT: It is well-known that all the phases of the manufacturing influence the extraordinary aesthetic and acoustic features of Stradivari's instruments. However, these masterpieces still keep some of their secrets hidden by the lack of documentary evidence. In particular, there is not a general consensus on the use of a protein-based ground coating directly spread on the wood surface by the Cremonese Master. The present work demonstrates that infrared scattering-type scanning near-fields optical microscopy (s-SNOM) may provide unprecedented information on very complex cross-sectioned microsamples collected from two of Stradivari's violins, nanoresolved chemical sensitivity being the turning point for detecting minute traces of a specific compound, namely proteins, hidden by the matrix when macro or micro sampling approaches are exploited. This nanoresolved chemical-sensitive technique contributed new and robust evidence to the long-debated question about the use of proteinaceous materials by Stradivari.

Elettra
Sincrotrone
Trieste

Materials science

MCX

ARTICLE

https://doi.org/10.1038/s41467-022-31768-5 OPEN

Development of vanadium-based polyanion positive electrode active materials for high-voltage sodium-based batteries

Semyon D. Shraer[1,2], Nikita D. Luchinin[1], Ivan A. Trussov[1], Dmitry A. Aksyonov[1], Anatoly V. Morozov[1], Sergey V. Ryazantsev[1,2], Anna R. Iarchuk[1], Polina A. Morozova[1], Victoria A. Nikitina[1,2], Keith J. Stevenson[1], Evgeny V. Antipov[1,2], Artem M. Abakumov[1] & Stanislav S. Fedotov[1]✉

Polyanion compounds offer a playground for designing prospective electrode active materials for sodium-ion storage due to their structural diversity and chemical variety. Here, by combining a $NaVPO_4F$ composition and $KTiOPO_4$-type framework via a low-temperature (e.g., 190 °C) ion-exchange synthesis approach, we develop a high-capacity and high-voltage positive electrode active material. When tested in a coin cell configuration in combination with a Na metal negative electrode and a $NaPF_6$-based non-aqueous electrolyte solution, this cathode active material enables a discharge capacity of 136 mAh g^{-1} at 14.3 mA g^{-1} with an average cell discharge voltage of about 4.0 V. Furthermore, a specific discharge capacity of 123 mAh g^{-1} at 5.7 A g^{-1} is also reported for the same cell configuration. Through ex situ and *operando* structural characterizations, we also demonstrate that the reversible Na-ion storage at the positive electrode occurs mostly via a solid-solution de/insertion mechanism.

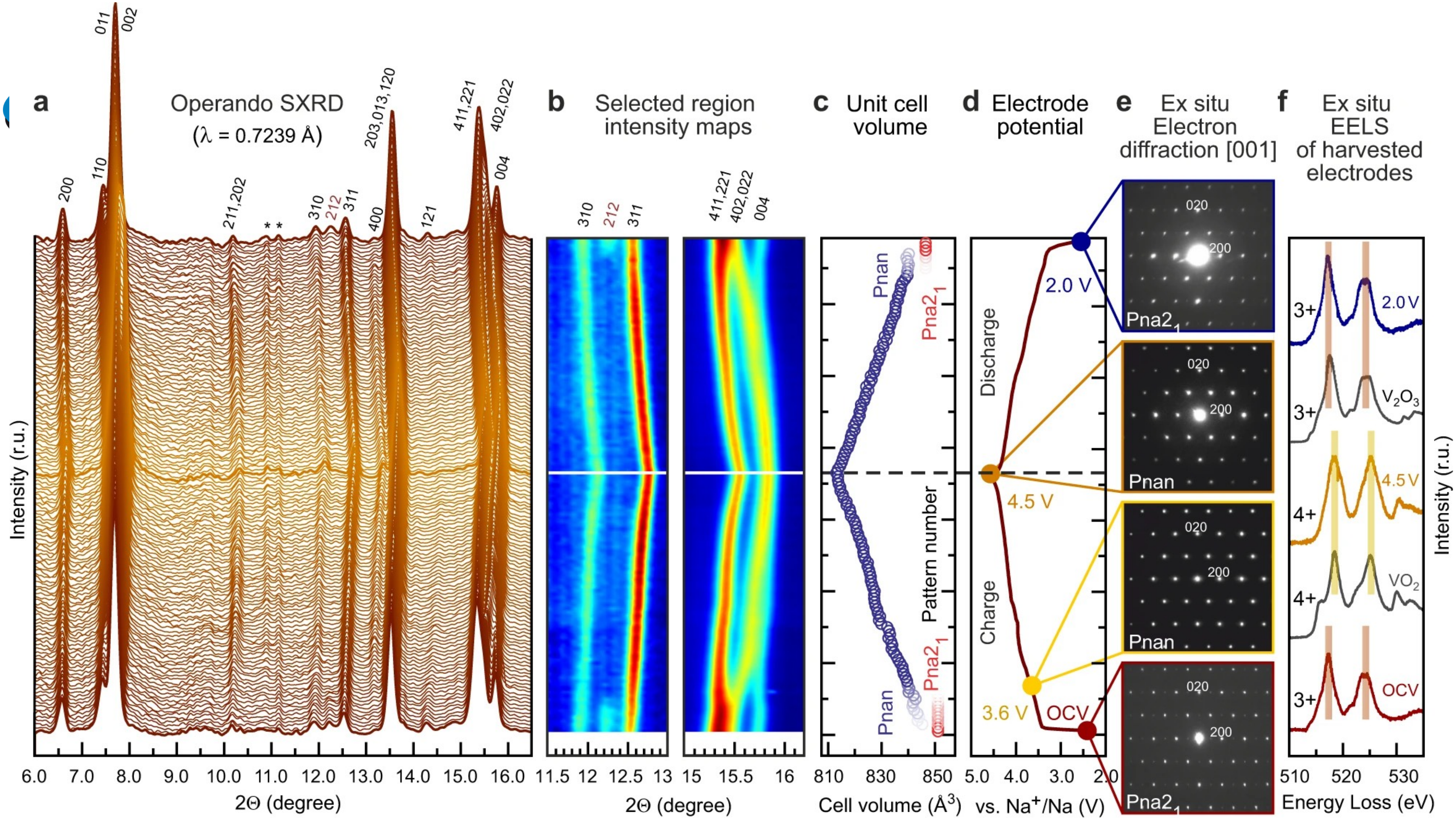

Structural evolution and charge compensation mechanism of $NaVPO_4F$ during cycling.

a Operando SXRD diffraction patterns in the 6.0–16.5° 2Θ range (λ = 0.7239 Å). The SXPD pattern highlighted in bold shows the charged phase. The asterisk sign (*) designates the reflections belonging to coin-cell components.

b Magnified regions of the *operando* SXRD intensity map. Horizontal full white and dashed black lines show the charged phase.

c Cell volume evolution on charge/discharge as refined from the operando SXRD data. Error bars are within the circles. Major ticks mark every 20th pattern.

d Corresponding charge-discharge profile in the Na||$NaVPO_4F$ cell, 1 M $NaPF_6$ in EC:PC:FEC (47.5:47.5:5 by vol.) electrolyte, the second cycle, measurements were conducted at 22 ± 2 °C.

e [001] ED patterns for the pristine material and recovered electrodes at 3.6, 4.5, and 2.0 V showing (dis) appearance of hk0: h + k = 2n + 1 reflections corresponding to the $Pna2_1$↔Pnan phase transition.

f Ex situ EELS spectra for the harvested electrodes at OCV, charged to 4.5 V, and discharged to 2.0 V manifesting the reversible change of vanadium oxidation state. The V2O3 and VO2 spectra are given for reference.

Life science

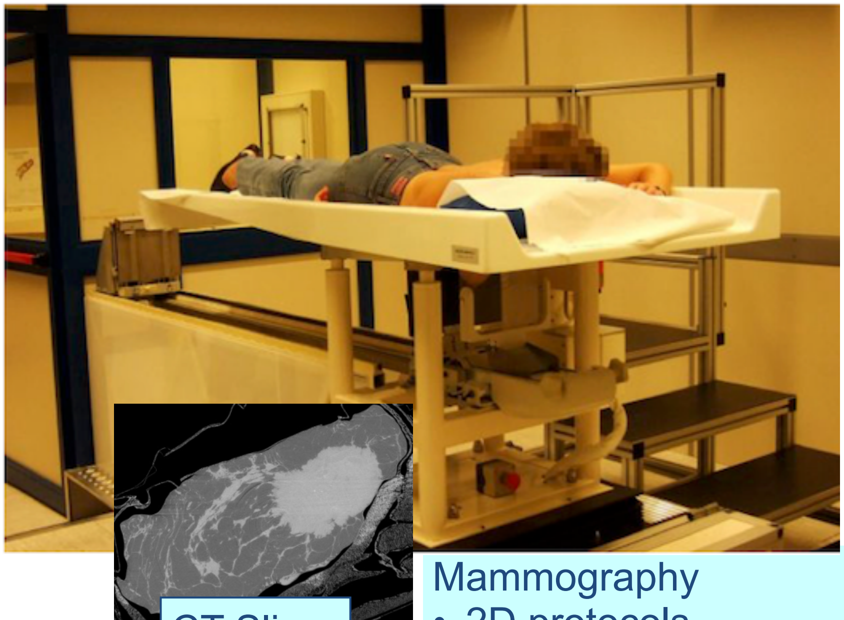

High-Res X-ray absorption and phase-contrast imaging (microtomography)

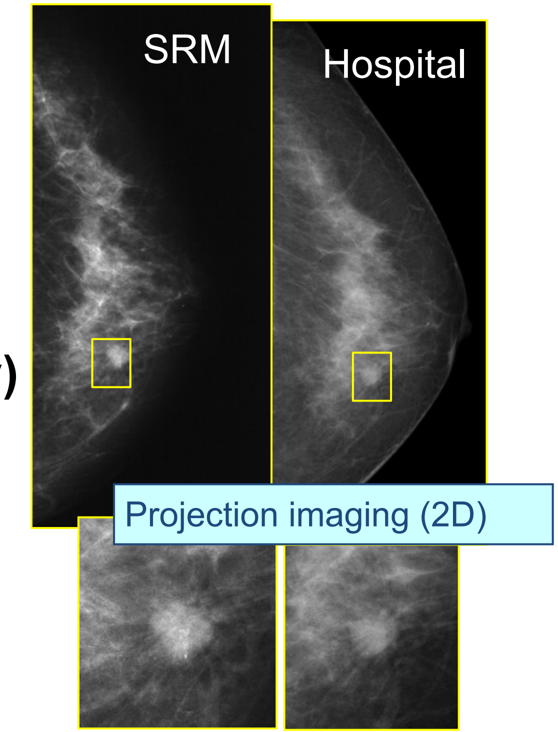

Mammography
- 2D protocols
- Low dose breast CT studies under evaluation

Pre-clinical and clinical phase contrast imaging (2D and 3D)
✓Cell tracking techniques
✓ Study of novel contrasts agents
✓Morphological and functional imaging
✓ Dynamic CT imaging (4D)
✓In-vivo imaging on small animal models
✓ **Breast imaging**

Clinical images with SR have:
- *higher specificity,*
- *better agreement with the golden standard (biopsy),*
- *improved image quality,*
- *strong reduction of X-ray doses.*

Morpho-mechanical characterisation of lung tissues of COVID patients

Different types of tissue damages are found in the same sample

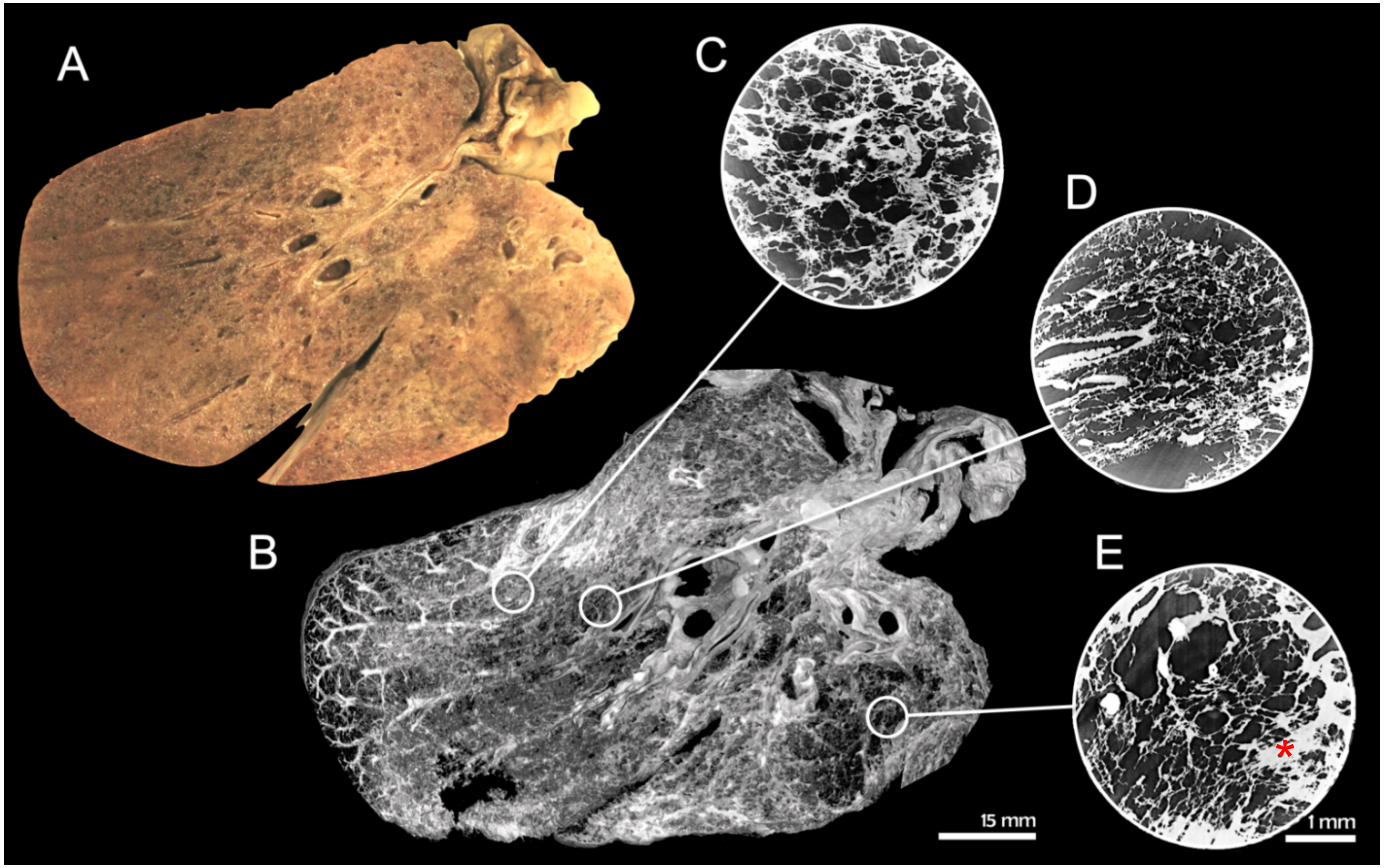

A) Picture of a Lamella
B) Global scan @ 100 µm resolution

C- E) Scan Zooms @ 5 µm:

- C) Expansion of alveolar ducts, thickening of interalveolar secta
- D) relatively preserved structure
- E) initial interstitial fibrosis

SYRMEP@Elettra
G. Tromba

Strategic international cooperation activities

- Training activities within the LAAAMP (Light sources for Africa, Americas, Asia, the Middle East and Pacific) initiative.

- Partnership with the International Atomic Energy Agency (IAEA) to run a BL for fluorescence with a focus on training of scientists from developing countries.

- Partnership with the International Center for Theoretical Physics (ICTP) to support users and training of scientists from developing countries.

- Partnership with the International Center for Genetic Engineering and Biotechnology (ICGEB) to support training of scientists from developing countries in the field of life sciences, with a focus on structural biology.

- MoU for technical training and support with SESAME.

- Pilot Action for training of young scientists from the Western Balkans.

Elettra is the Italian representing entity and Partner Facility within CERIC-ERIC, the Center European Research Infrastructure Consortium, which includes laboratories from:

- Austria
- Croatia
- Czech Republic
- Hungary
- Poland
- Slovenia
- Romania

Elettra Sincrotrone Trieste

The future: Elettra 2.0

Elettra 2.0 Lattice

Exploiting multi-bend technology to approach the theoretical brightness limit - the third European upgrade project

Going from the Elettra double bend achromat lattice (left) to the Elettra 2.0 symmetric six-bend enhanced achromat lattice (right)

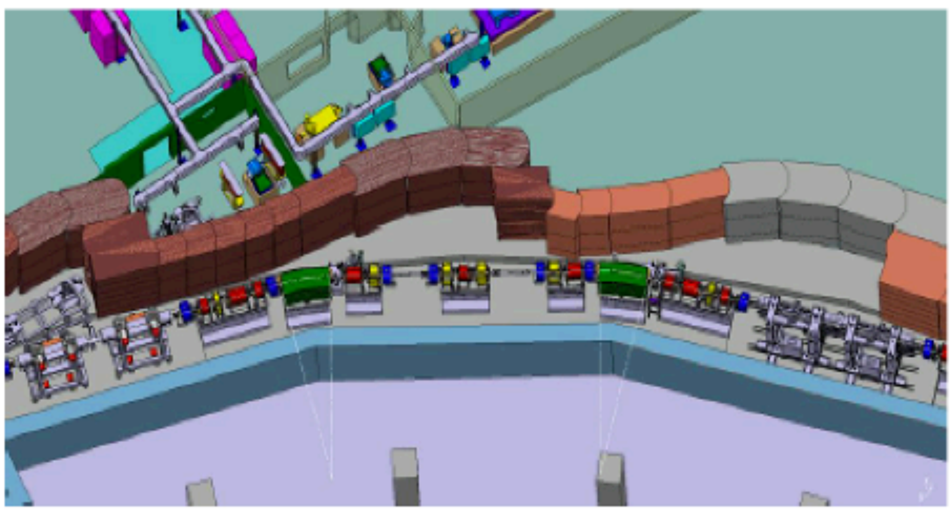

Elettra

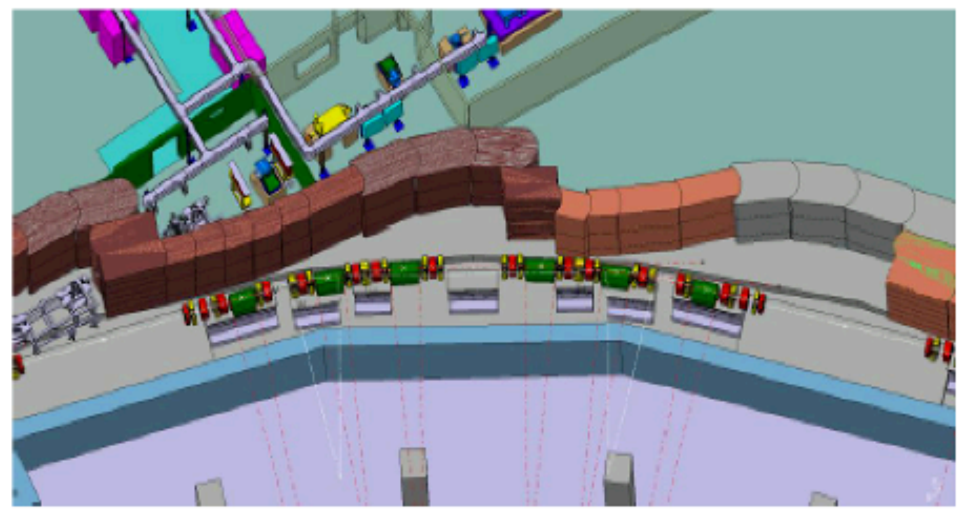

Elettra 2.0

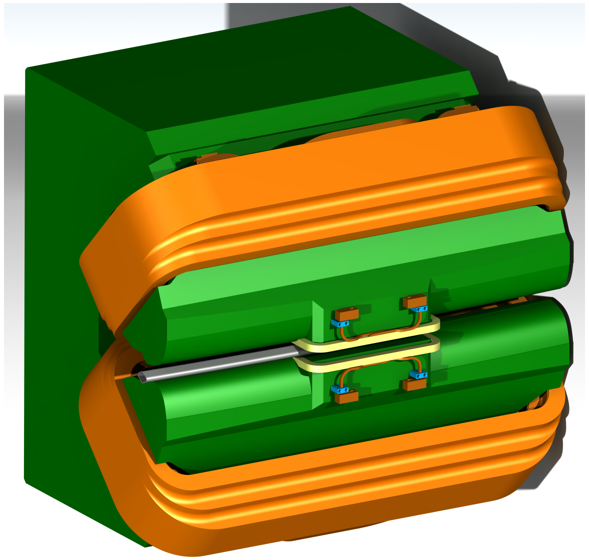

Special longitudinal and transverse gradient dipole

Strong 50 T/m quadrupole

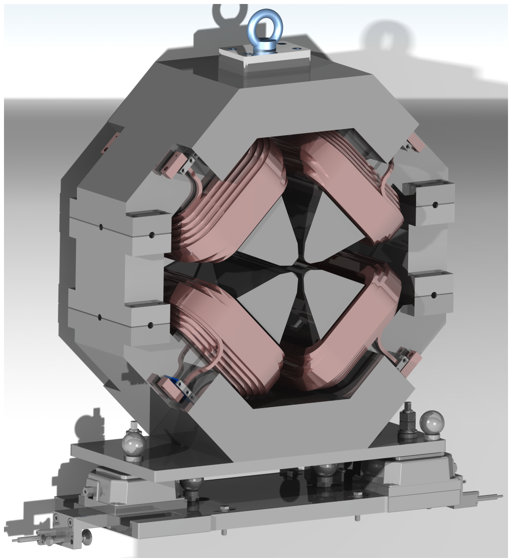

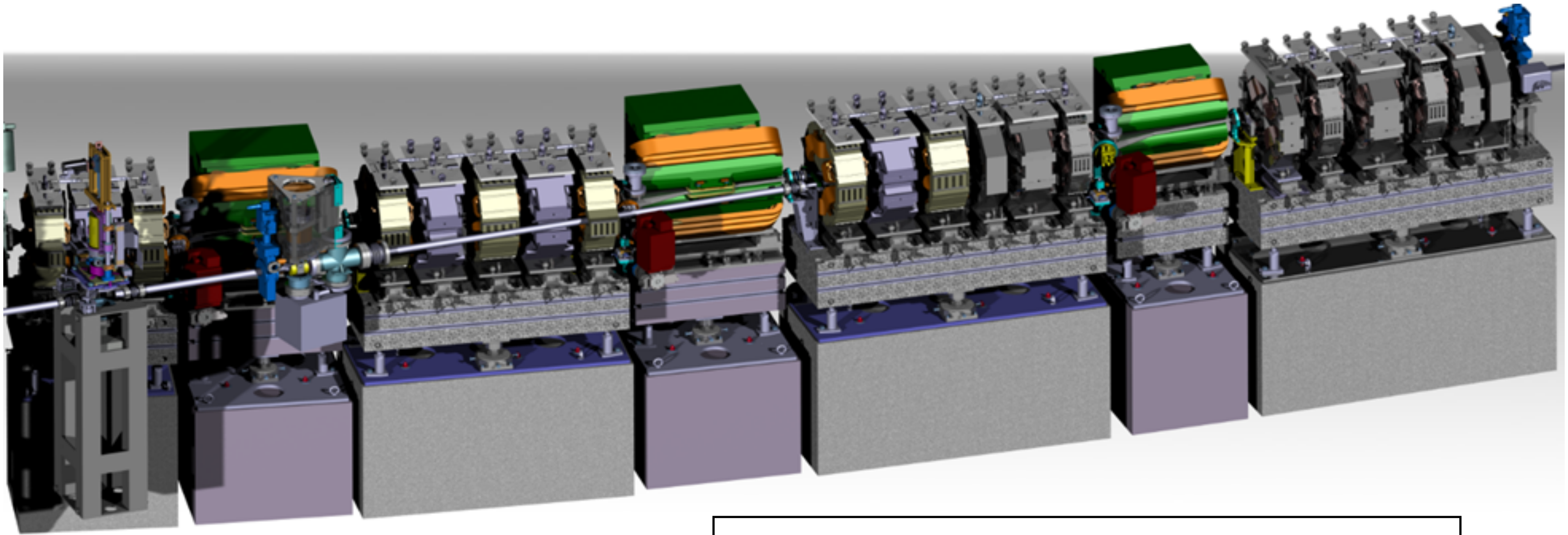

Elettra 2.0 half achromat with magnets, girders and light exits

Elettra Sincrotrone Trieste

Elettra 2.0: scope and strategy

➢ **Scope of the project**

- maintaining the Elettra synchrotron light laboratory at the forefront of synchrotron user facilities in a broad photon energy window ranging from IR and THz to the hard X-rays;
- increasing the capacity of the laboratory to attract new user communities.

➢ **Strategy**

- Designing of a suite of new beamlines exploiting the improvement opportunities of the new source (increased coherence in soft/hard-X and brilliance, increased time-resolution (possibly ps), in-vacuum undulators);
- merging of some beamlines;
- upgrading some beamlines maintained on Elettra 2.0 for having better performance;
- relocation of existing beamlines where required;
- removal of some beamlines;
- upgrade of the instrumentation for new science and users.

Elettra
ID photon
spot size

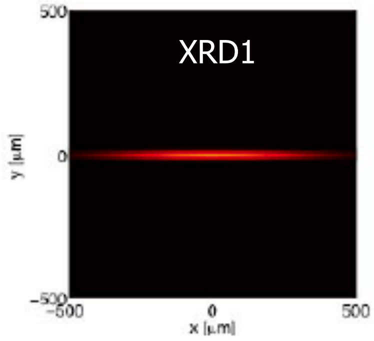

ELETTRA 2.0

1000 TIMES BRIGHTER
50 TIMES MORE COHERENT

Elettra 2.0
ID photon
spot size

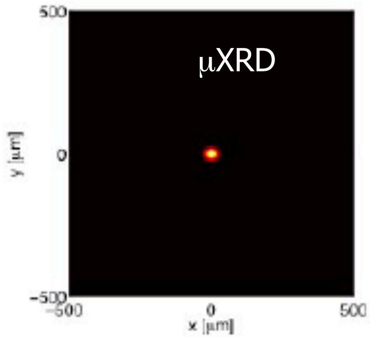

Parameter	Units	Elettra	Elettra 2.0 S6BA-E
Circumference	m	259.2	259.2
Energy	GeV	**2.4**	**2.4**
Horizontal bare emittance	pm rad	10000	212
Vertical emittance @1% coupling	pm rad	100	2.1
Beam size @ ID (sx,sy)	um	286 , 16	36 ,1.5
Beam size at short ID	um	400 , 25	64, 2.2
Beam size @ Bend (at z=0)	um	272, 27	8 , 6
Bunch length (zero current, 2 MV,1s)	ps	22	5.4
Energy spread	DE/E %	0.095	0.11

Elettra Sincrotrone Trieste

Science Drivers of Elettra 2.0

Reduction in the **source emittance** and **beam size** and the **brightness** increase will lead to:

➢significant ***gains in the emitted or transmitted signals*** from the objects under investigation;
➢***reduced acquisition time*** for all types of spectroscopies and X-ray scattering techniques;
➢implementation of ***photon-hungry techniques*** such as: high pressure experiments with anvil cells and dilute samples and spin-resolved ARPES;
➢improvement of the ***lateral resolution*** with focusing optics down to a few nm scale range (e.g. nano-PES, nano-ARPES)

The high **coherence** will open unique opportunities for coherence-hungry methods:

➢***Coherent Diffraction Imaging*** (CDI) with chemical specificity
➢***Ptychography***
➢***X-ray photon correlation spectroscopy*** (XPCS)

Elettra Sincrotrone Trieste

Science Drivers of Elettra 2.0
(Snapshots from the TDR)

Condensed matter

❑ Correlated systems and magnetism

X-ray photon correlation spectroscopy (XPCS)

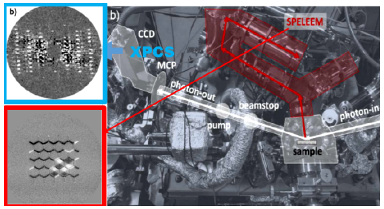

The new HB-SAXS for XPCS in the hard X-rays

XPEEM-XPCS set-up at Nanospectroscopy, tested in 2020

Coherent diffraction imaging

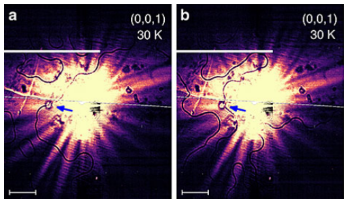

Antiferromagnetic arrangements imaging @CSX-NSLS-II

The new CDI beamline for soft and tender X-ray coherent scattering and imaging

Spin-ARPES spectroscopy and spectromicroscopy

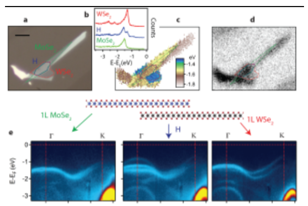

Band parameters and hybridization in 2D semiconductor heterostructures @ Spectromicroscopy

❑ Functional materials for catalysis, energy conversion and storage

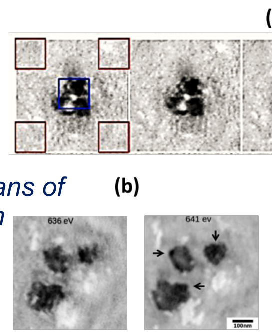

Absorption and ptychographic scans of a Mn–Co/PPy film @TwinMic

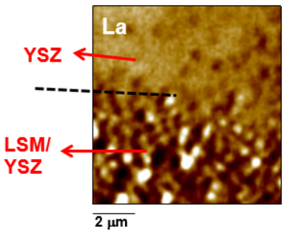

Spatially resolved NAP-XPS of SOFC electrode-electrolyte interface @ ESCA Microscopy

Life sciences

❑ From Protein Science to Cellular Biology

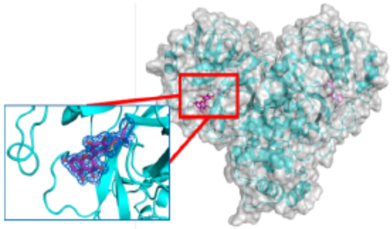

3D structure of SARS-CoV-2 Mpro in complex with myricetin

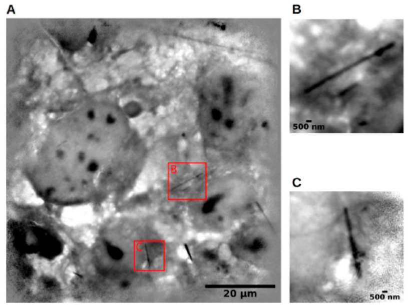

Ptychographic phase reconstruction of mesothelial cells @ TwinMic

A brand new class of microscopes for MX, XRF, XAS, SAXS, Ptychography

❑ Medical imaging

Lung CT@Syrmep

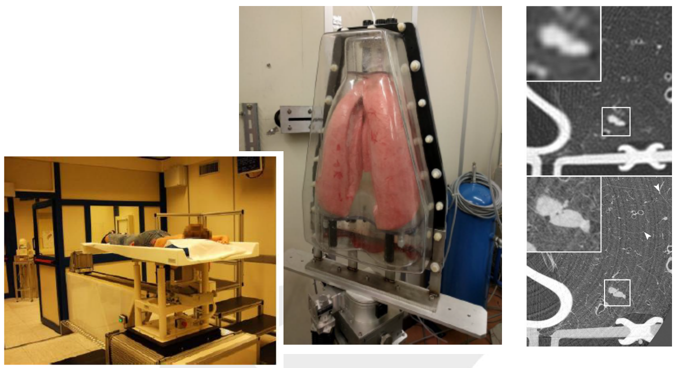

Syrmep-LS: a dedicated beamline and patient room

CERTIFIED MANAGEMENT SYSTEM
CQY CERTIQUALITY
UNI EN ISO 9001:2015
UNI ISO 45001:2018

The SYRMEP – Life Science beamline

Higher energies for multiscale and multi resolution tomography and imaging applications

(Giuliana Tromba & Diego Dreossi)

- "In vitro" imaging: high resolution morphological studies (es. micro-CT studies of tissues, organs, biomaterials - virtual histology)
  High resolution required, main limitation is radiation damage, typical pixel size:0.9-3 μm

- Imaging of small animals ('Pre-clinical'): applied for different purposes in the development of ***animal models***
  Research protocols, pixel size: 9 μm (for ex-vivo) up to 100 μm (in-vivo).

- Clinical: applications to patients
  *Need to **limit** radiation dose. Strict research protocol for selected patients. Find best compromise between dose and image quality, pixel sizes : 50 – 100 μm*

EURO-BIOIMAGING

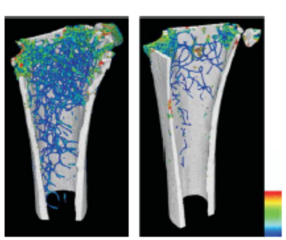

UNI EN ISO 9001:2015
UNI ISO 45001:2018

breast CT

lung CT

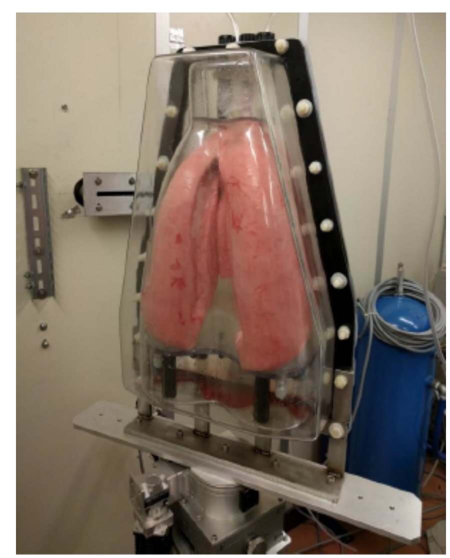

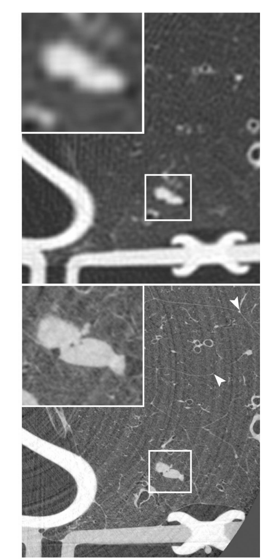

Elettra Sincrotrone Trieste

The SYRMEP – Life Science beamline

A superconducting bending magnet with peak magnet field of 6 T is planned (critical energy at 2.4 GeV = 23 keV)

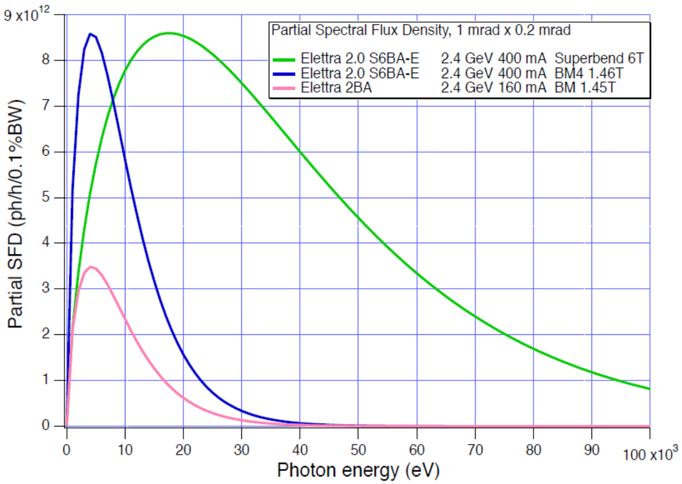

	High resolution /Multiple scale CT				Medium resol./ pre-clinical in-vivo low dose	Clinical - Breast, cartilages	Pre-clinical big animals Clinical - Lung
	Max res (High res Zoom CT)	In-situ (2 scales)	Static	4D			
Sample hor. size/thickness	1 - 5 mm	5 - 10 mm or 10 - 50 mm	5 - 30 mm or 50 - 300 mm	5 - 30 mm or 50 - 300 mm	20 – 50 mm	6 - 15 cm	> 30 cm
Requirements for sample vertical sizes (including support)	< 50 mm	20-30 + *in-situ* device, bigger sizes in case of human samples (bones)	up to 300 (long samples setup for botanic applications))	20-40 mm or 50-300 mm	30 - 300 mm + sample support	< 15 cm	> 30 cm
Typical needed FOVs	3 - 6 mm	1.8 - 10.2 mm 10.2 - 150 mm or more	1.8 - 10.2 mm 6.1 - 150 mm or more	1.8 - 10.2 mm 6.2 - 150 mm or more	30 - 50 mm	> 15 cm (covers the beam size)	> 15 cm (covers the beam size)
Energy range (keV)	10-40	10-40	10-60	10-60	17-35	18-60	> 60
Imaging modes	FP KES, Spectral imaging	FP KES, Spectral imaging	FP KES, Spectral imaging ABI, and others	FP KES, Spectral imaging ABI, and others	FP KES ABI, and others	FP ABI or Others	FP
Typical FP dist. (m)	0 - 0.7 m	0 - 1.5 m	0 - 1.5 m or 0 - 6 m	0 - 1.5 m or 0 - 6 m	0 – 3 m	≥ 9 m	> 9 m

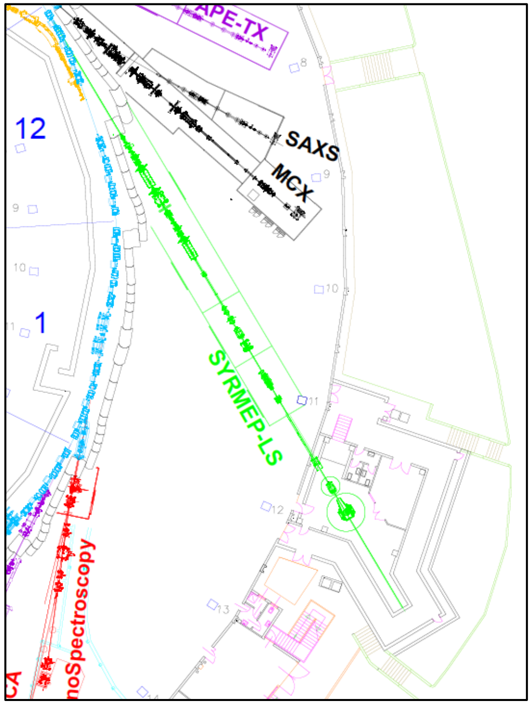

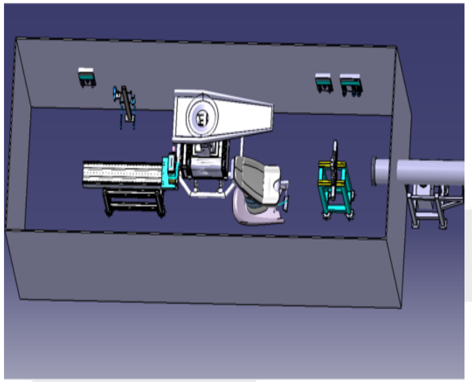

Status of the project (installation on Elettra 1.0 - 2024)

Source — *SBM tech specifications ready*

Beamline — *Contract signed end 2022*

Patients room — *Preliminary studies ongoing (Elettra Infrastructure Service)*

Master time plan for the preparation and installation of the beamlines

- ➢ Anticipate possible upgrades before the dark period
- ➢ Use the long machine shutdowns
- ➢ Follow priorities
- ➢ Avoid shutdowns of beamlines activities

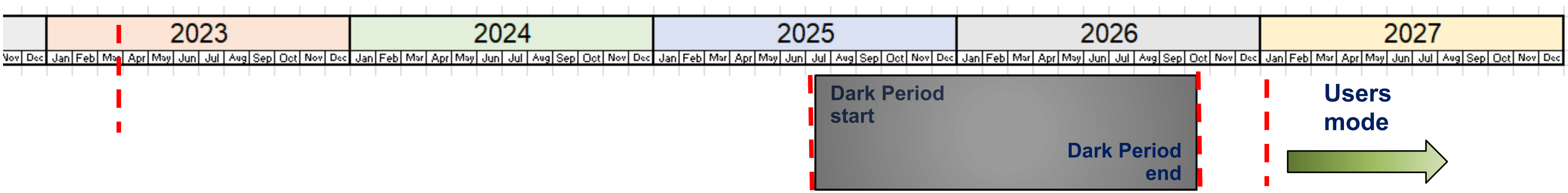

PHASE 1 *(all beamlines in operation)*

Main activities:

- ➢ Upgrade of the Beamline Control System
- ➢ Upgrade of the Personal Safety System
- ➢ Replace wherever needed of the first optics cooling system
- ➢ Upgrade wherever needed of the safety hutches
- ➢ Installation of SYRMEP-LS and HF-SAXS (space already available)
- ➢ Removal of SR-FEL and LILIT
- ➢ Adjustment of the tunnel wall where possible

PHASE 2

- ➢ Installation of most of the new beamlines
- ➢ Upgrade of the liquid nitrogen distribution plant
- ➢ Completion of the tunnel wall adjustment

PHASE 3

- ➢ Installation of the remaining beamlines

Elettra
Sincrotrone
Trieste

Elettra
Sincrotrone
Trieste

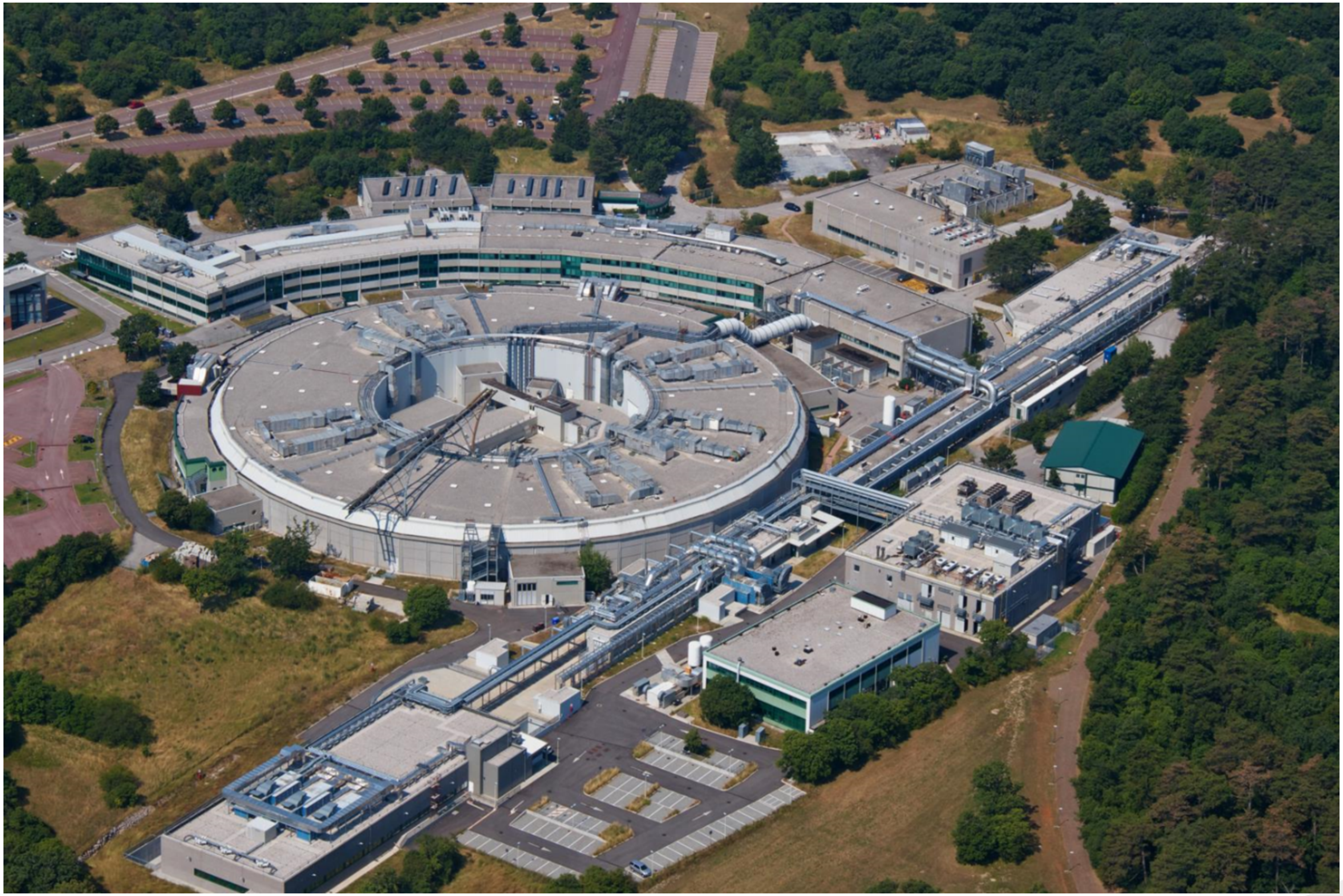

Elettra
Sincrotrone
Trieste

Elettra 2.0-2.4 GeV 3rd generation Synchrotron Radiation Facility

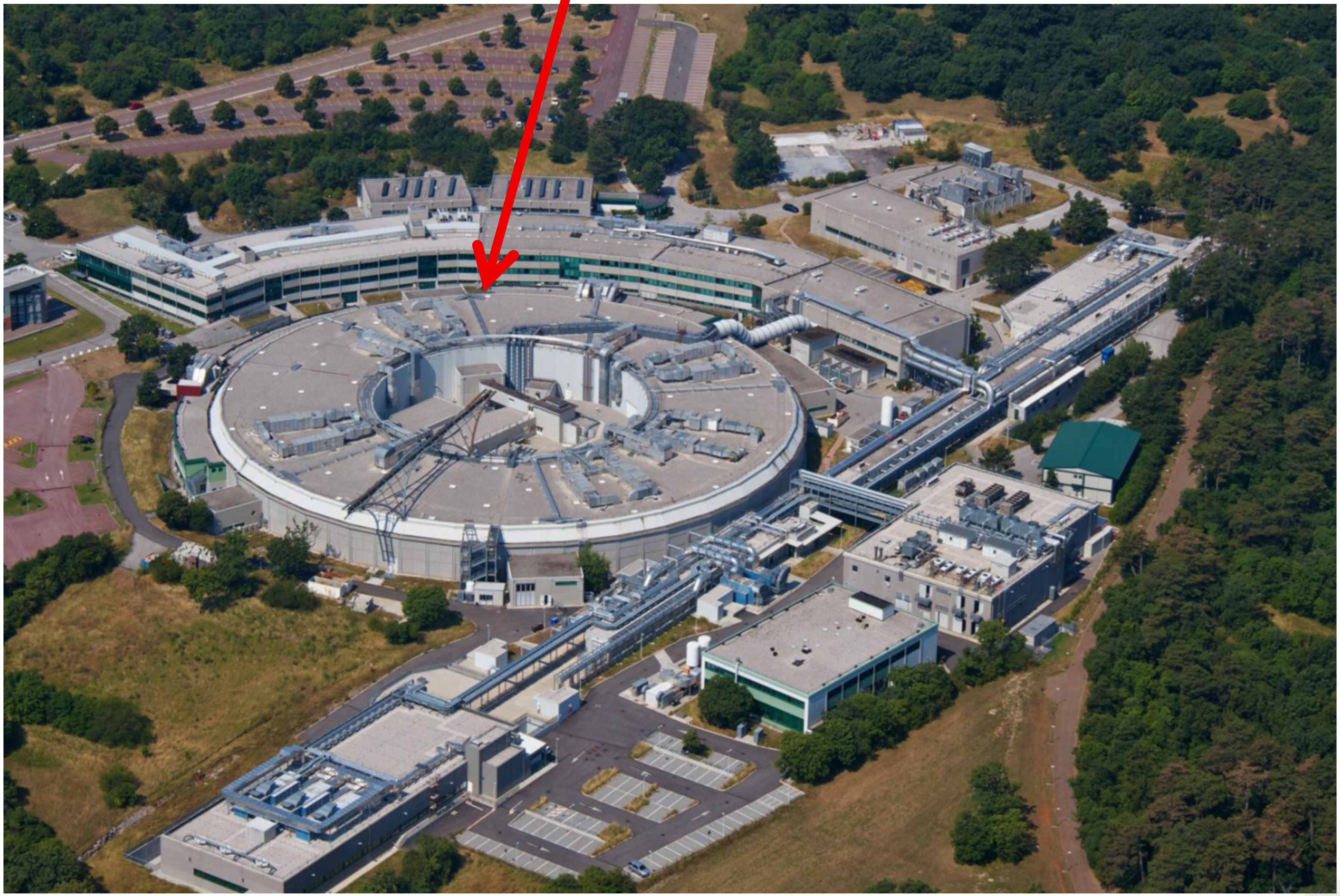

CERTIFIED MANAGEMENT SYSTEM
CQY CERTIQUALITY
UNI EN ISO 9001:2015
UNI ISO 45001:2018

Elettra 2.0-2.4 GeV 3rd generation Synchrotron Radiation Facility

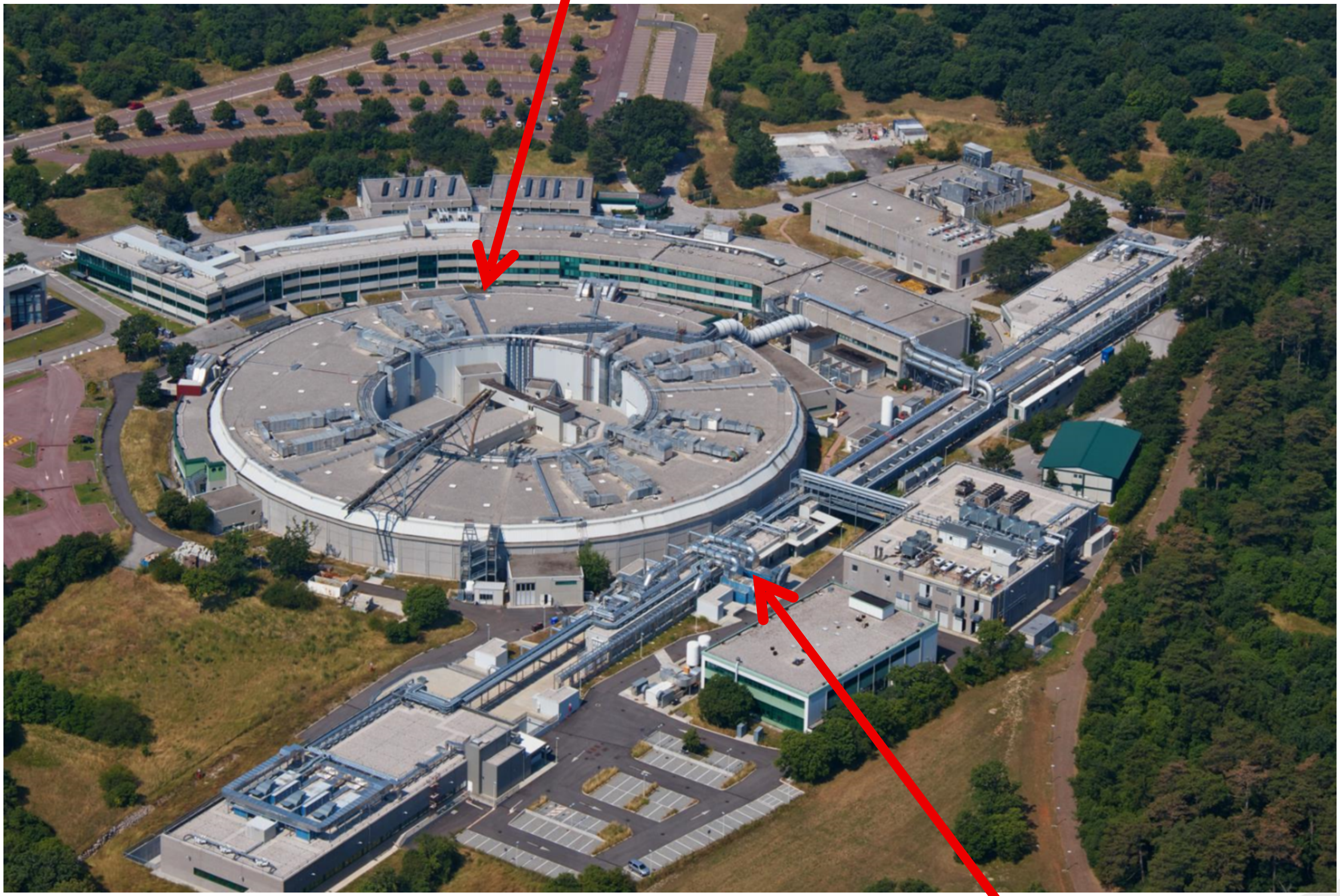

FERMI 1.5 GeV seeded Free Electron Laser Facility

Elettra Sincrotrone Trieste

Elettra 2.0-2.4 GeV 3rd generation Synchrotron Radiation Facility

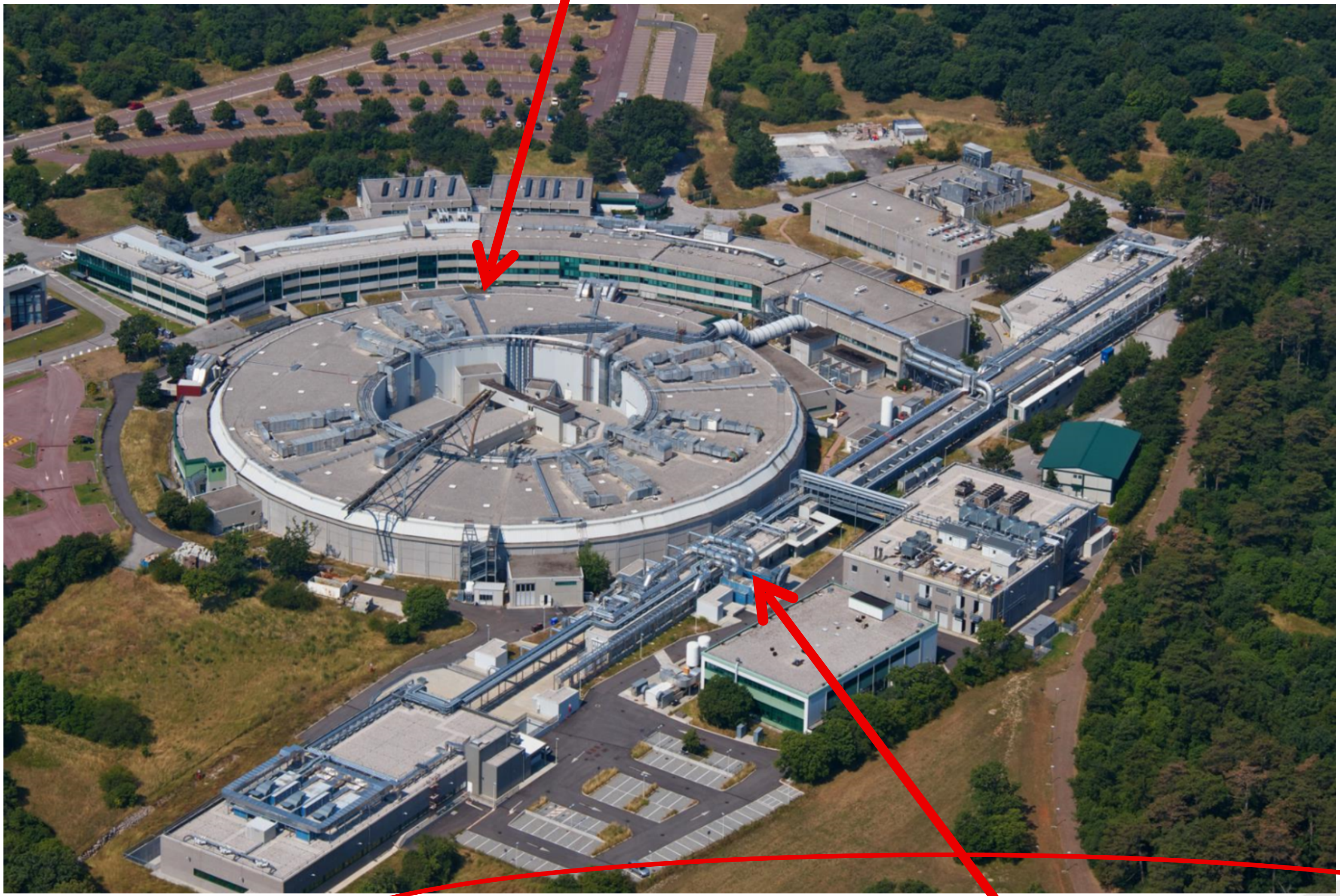

FERMI 1.5 GeV seeded Free Electron Laser Facility

CERTIFIED MANAGEMENT SYSTEM
CQY CERTIQUALITY
UNI EN ISO 9001:2015
UNI ISO 45001:2018

FEL microbunching

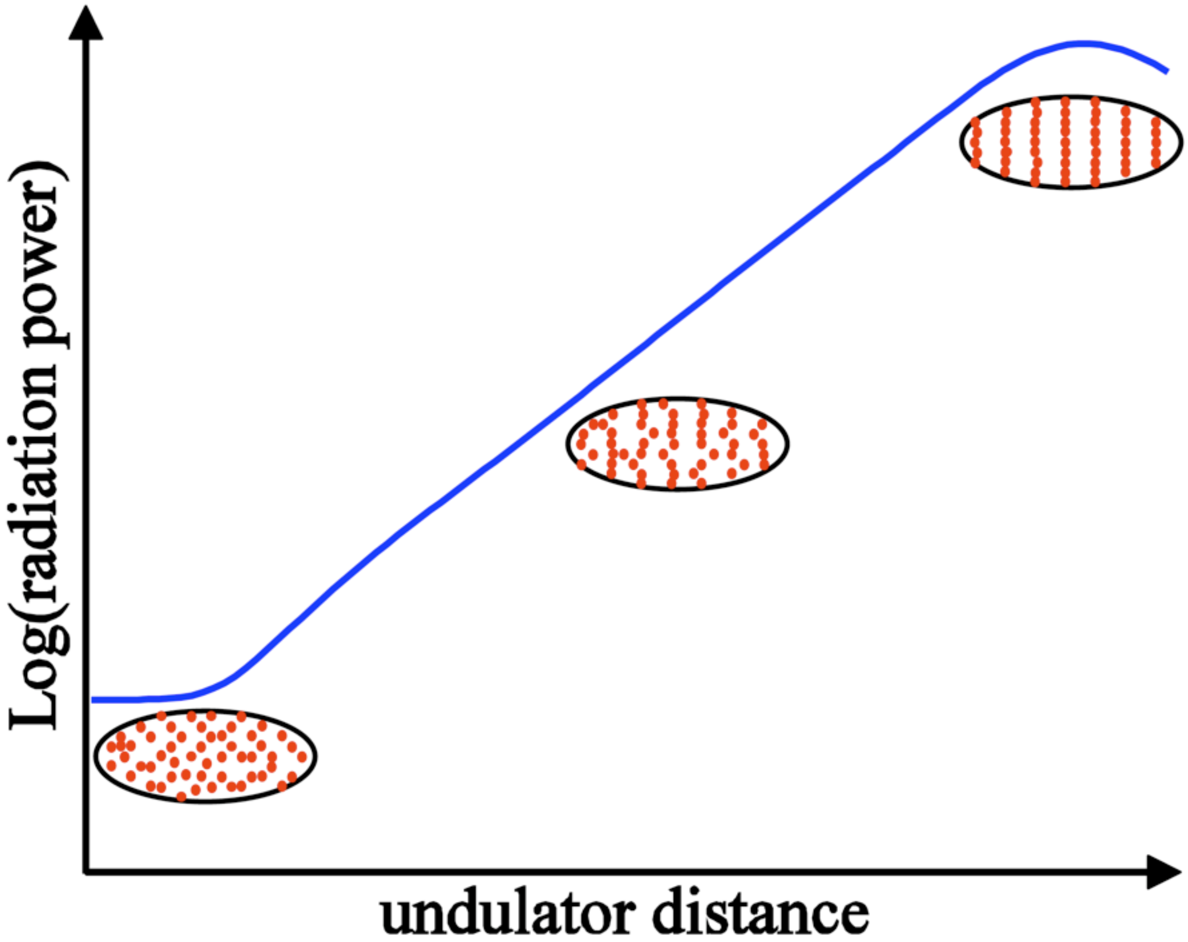

Growth of the radiation power and the electron beam microbunching as a function of the undulator distance for a high-gain FEL.

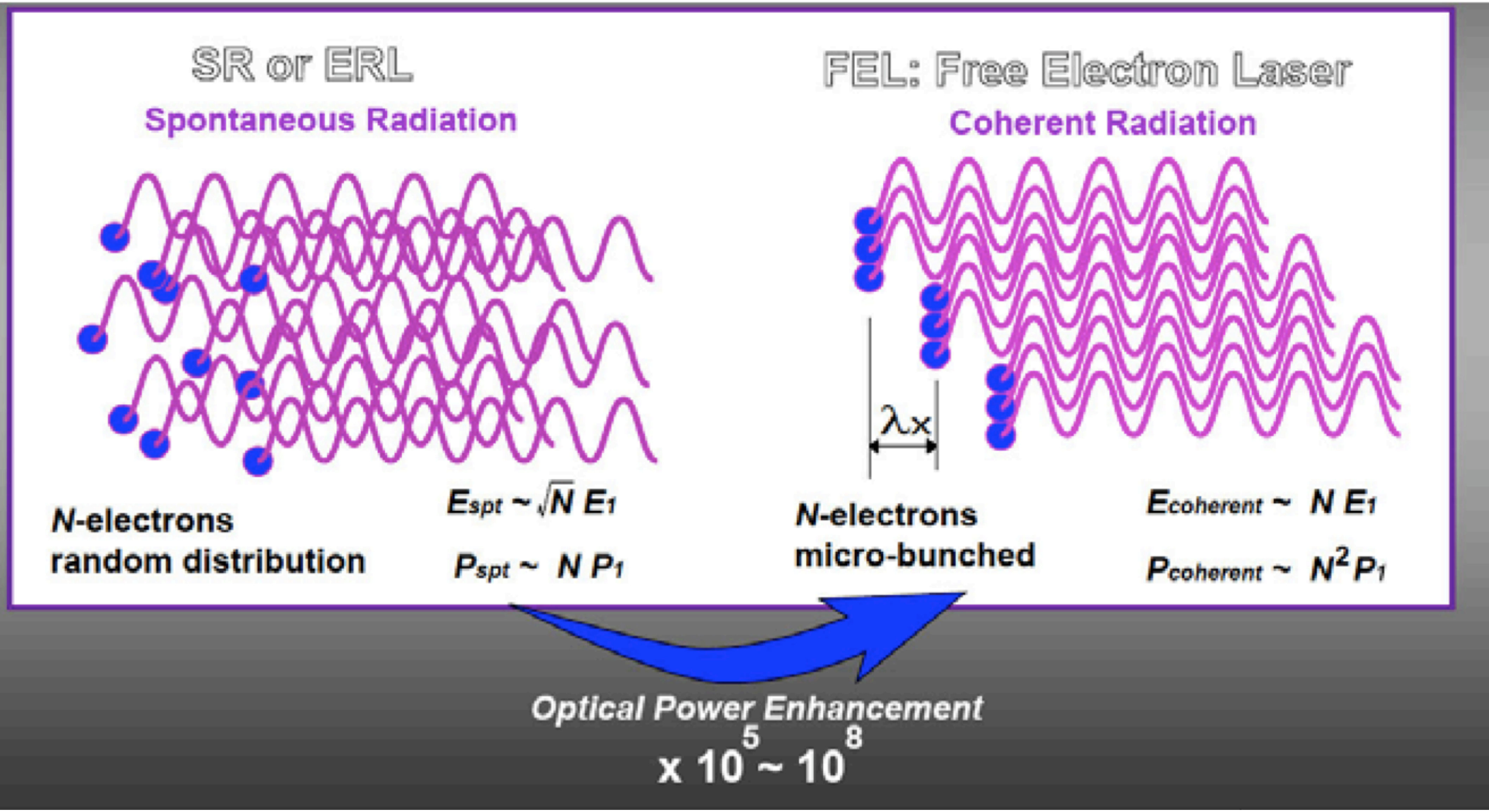
SR or ERL
Spontaneous Radiation
FEL: Free Electron Laser
Coherent Radiation
λx
N-electrons
random distribution
$E_{spt} \sim \sqrt{N}\, E_1$
$P_{spt} \sim N P_1$
N-electrons
micro-bunched
$E_{coherent} \sim N E_1$
$P_{coherent} \sim N^2 P_1$
Optical Power Enhancement
$\times\, 10^5 \sim 10^8$

Overall length of underground part (5 m below ground): ~ 400 m
Three main parts: Linac & Klystron Hall; Undulator Hall; Experimental Hall

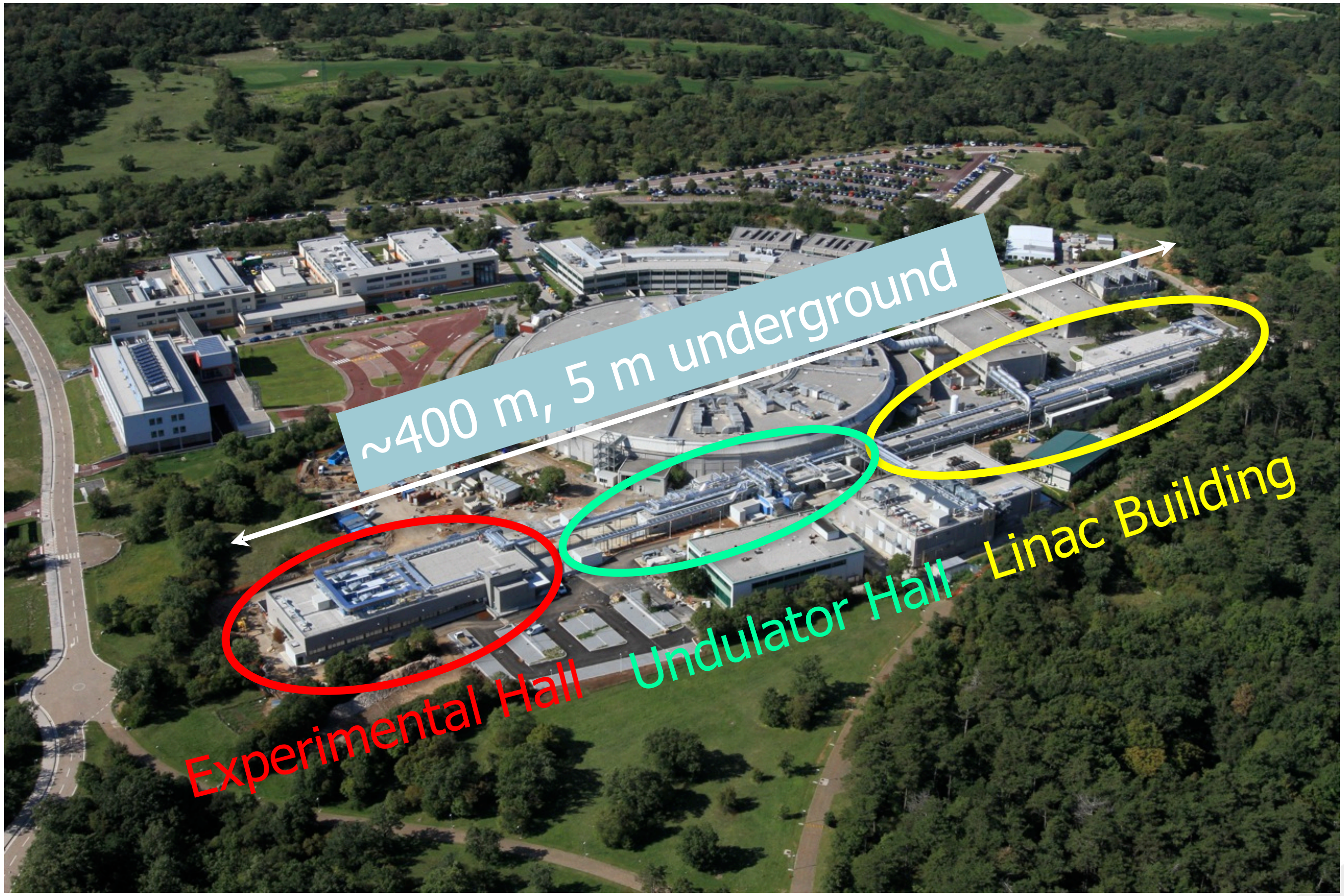

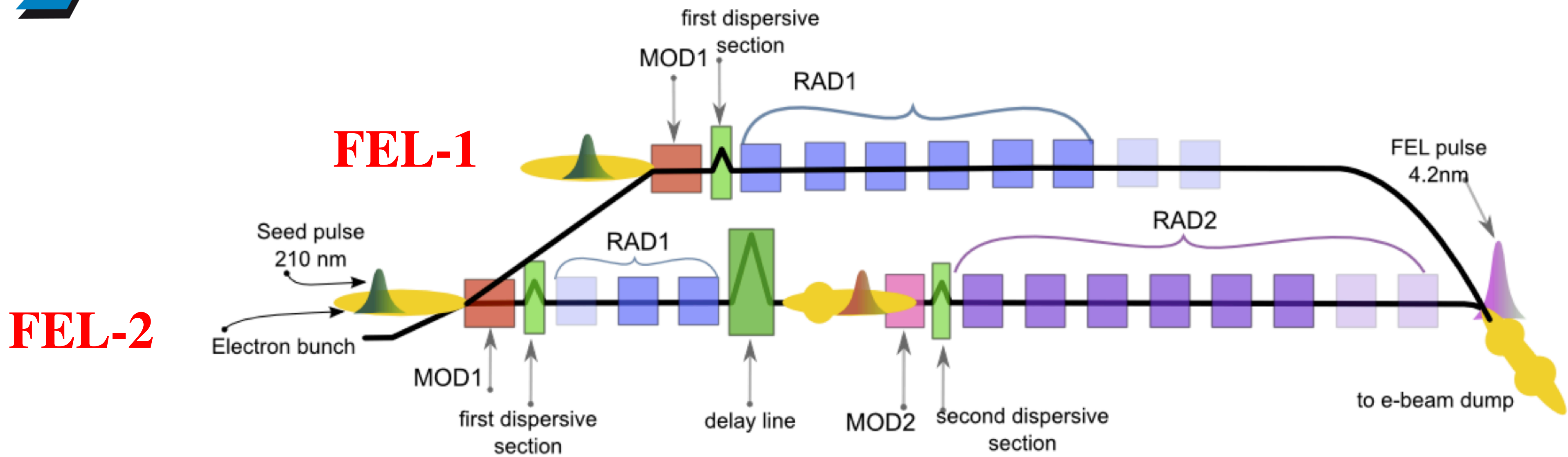
FEL-1
FEL-2
first dispersive
section
MOD1
RAD1
FEL pulse
4.2nm
Seed pulse
210 nm
RAD1
RAD2
Electron bunch
MOD1
first dispersive
section
delay line
MOD2
second dispersive
section
to e-beam dump

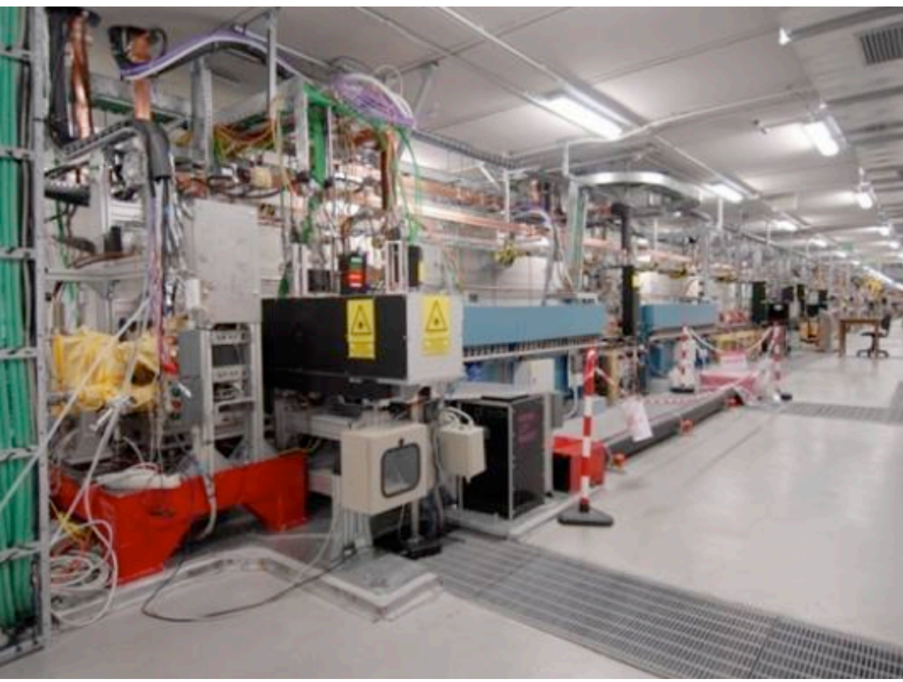

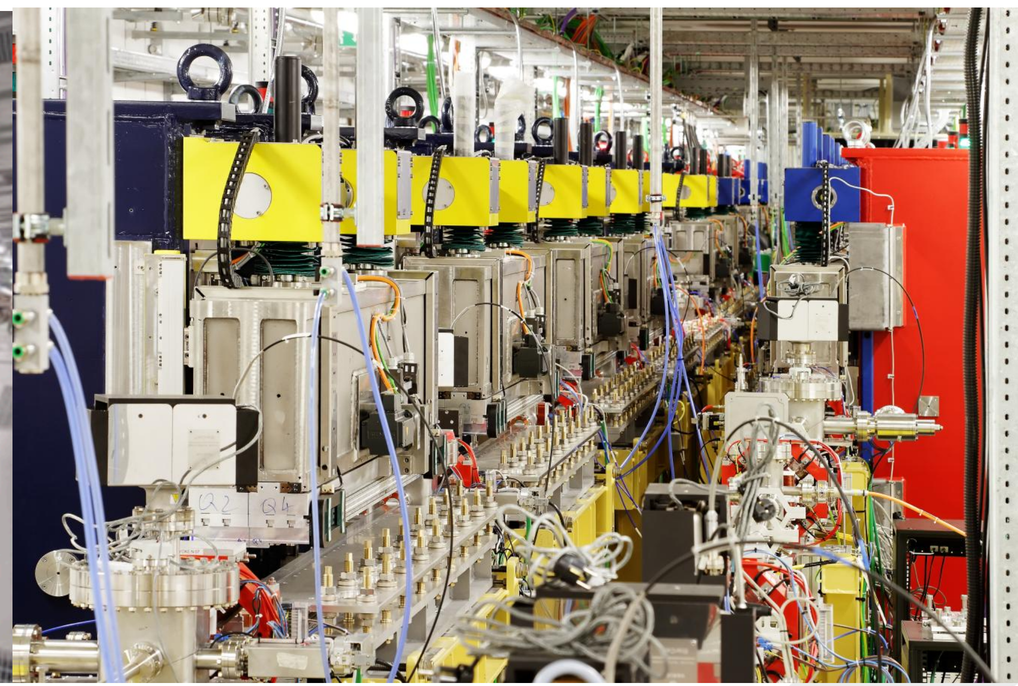

Elettra
Sincrotrone
Trieste

A liquid carbon (l-C) sample is generated through constant volume heating exposing an amorphous carbon foil to an intense ultrashort laser pulse. Time-resolved x-ray absorption spectroscopy at the C K edge is used to monitor the dynamics of the melting process revealing a subpicosecond rearrangement of the electronic structure associated with a sudden change of the C bonding hybridization. The obtained l-C sample, resulting from a nonthermal melting mechanism, reaches a transient equilibrium condition with a temperature of about 14 200 K and pressure in the order of 0.5 Mbar in about 0.3 ps, prior to hydrodynamic expansion. A detailed analysis of the atomic and electronic structure in solid-density l-C based on time-resolved x-ray absorption spectroscopy and theoretical simulations is presented. The method can be fruitfully used for extending the experimental investigation of the C phase diagram in a vast unexplored region covering the 103–104 K temperature range with pressures up to 1 Mbar.

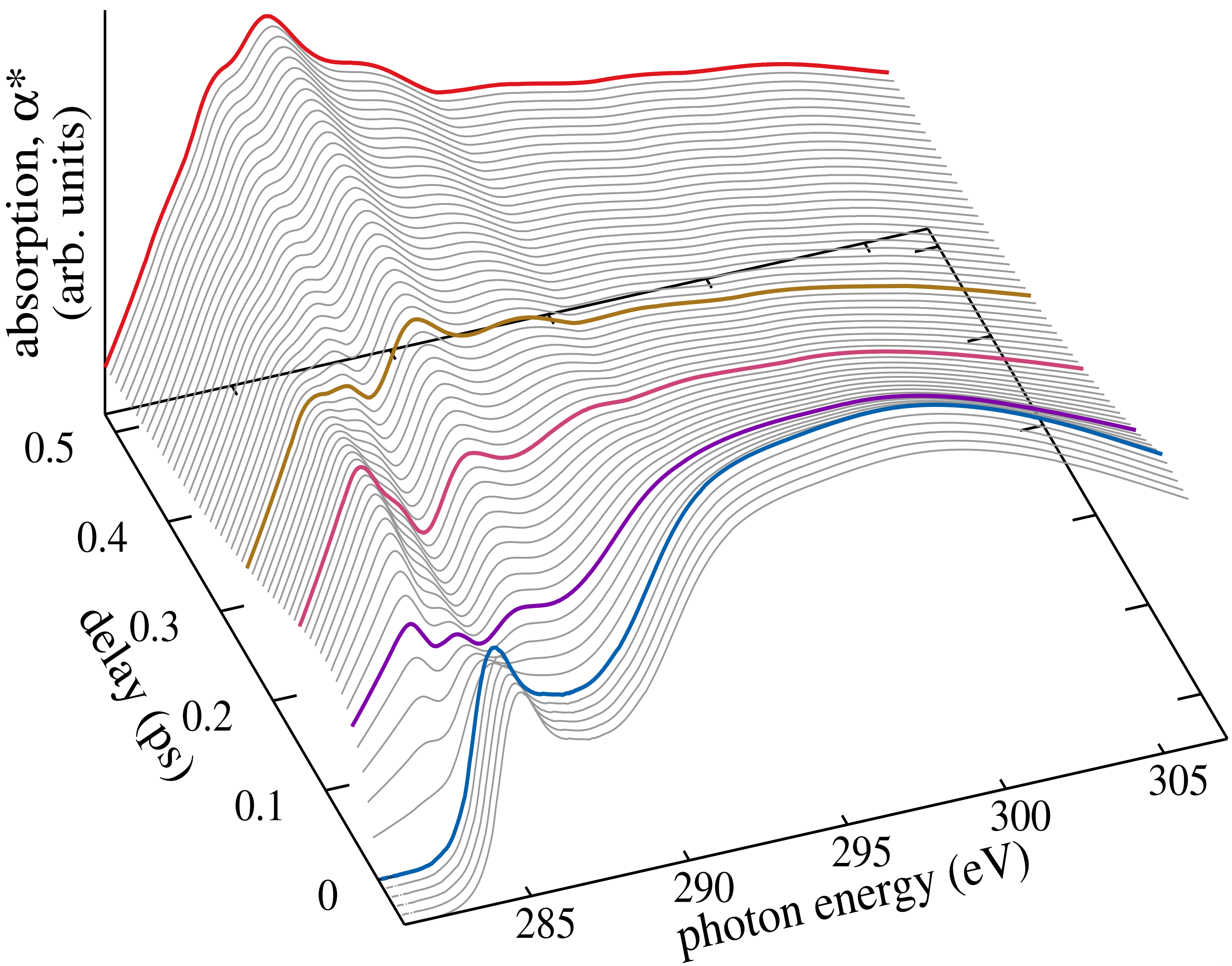

A liquid carbon (l-C) sample is generated through constant volume heating exposing an amorphous carbon foil to an intense ultrashort laser pulse. Time-resolved x-ray absorption spectroscopy at the C K edge is used to monitor the dynamics of the melting process revealing a subpicosecond rearrangement of the electronic structure associated with a sudden change of the C bonding hybridization. The obtained l-C sample, resulting from a nonthermal melting mechanism, reaches a transient equilibrium condition with a temperature of about 14 200 K and pressure in the order of 0.5 Mbar in about 0.3 ps, prior to hydrodynamic expansion. A detailed analysis of the atomic and electronic structure in solid-density l-C based on time-resolved x-ray absorption spectroscopy and theoretical simulations is presented. The method can be fruitfully used for extending the experimental investigation of the C phase diagram in a vast unexplored region covering the 103–104 K temperature range with pressures up to 1 Mbar.

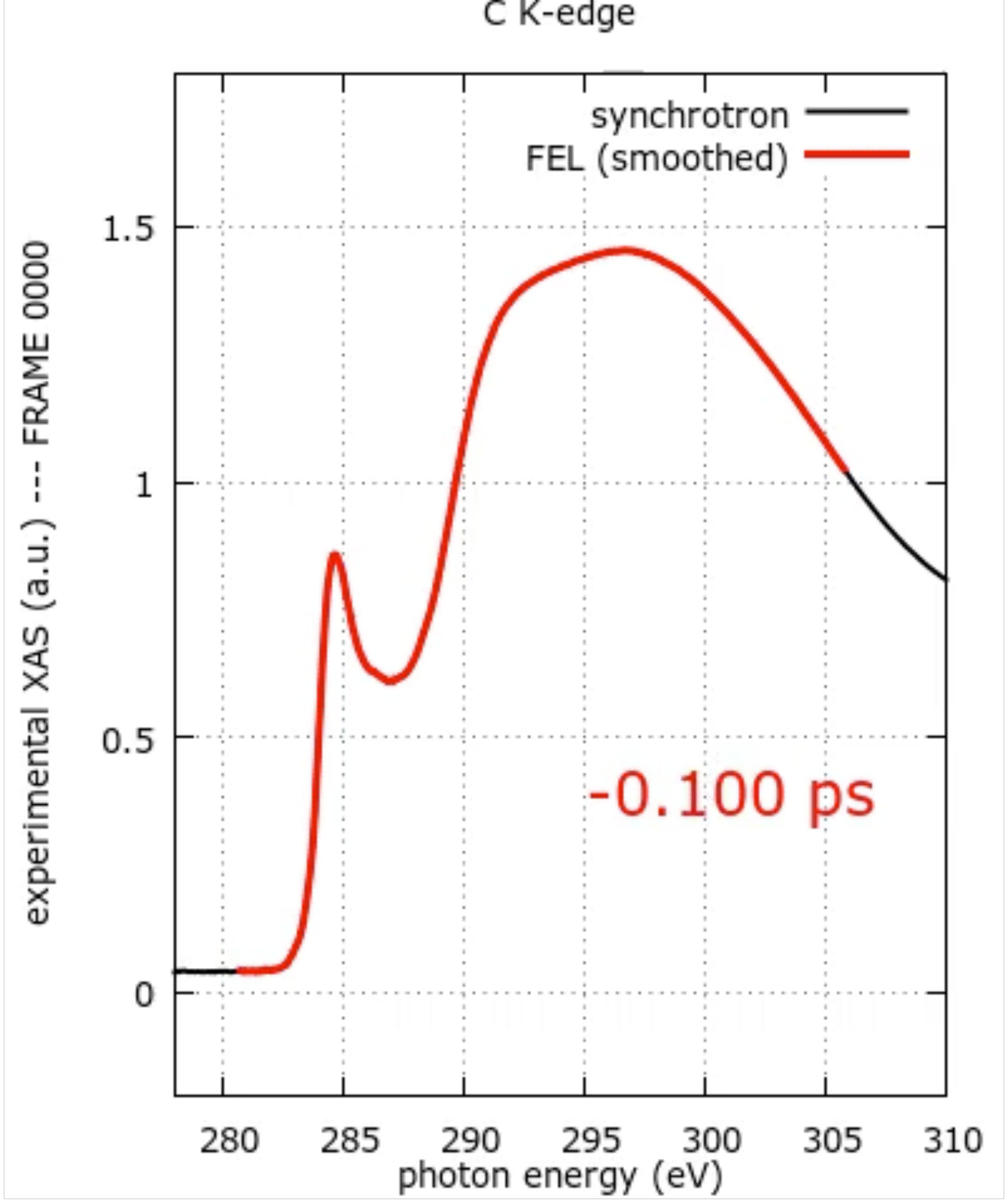

A liquid carbon (l-C) sample is generated through constant volume heating exposing an amorphous carbon foil to an intense ultrashort laser pulse. Time-resolved x-ray absorption spectroscopy at the C K edge is used to monitor the dynamics of the melting process revealing a subpicosecond rearrangement of the electronic structure associated with a sudden change of the C bonding hybridization. The obtained l-C sample, resulting from a nonthermal melting mechanism, reaches a transient equilibrium condition with a temperature of about 14 200 K and pressure in the order of 0.5 Mbar in about 0.3 ps, prior to hydrodynamic expansion. A detailed analysis of the atomic and electronic structure in solid-density l-C based on time-resolved x-ray absorption spectroscopy and theoretical simulations is presented. The method can be fruitfully used for extending the experimental investigation of the C phase diagram in a vast unexplored region covering the 103–104 K temperature range with pressures up to 1 Mbar.

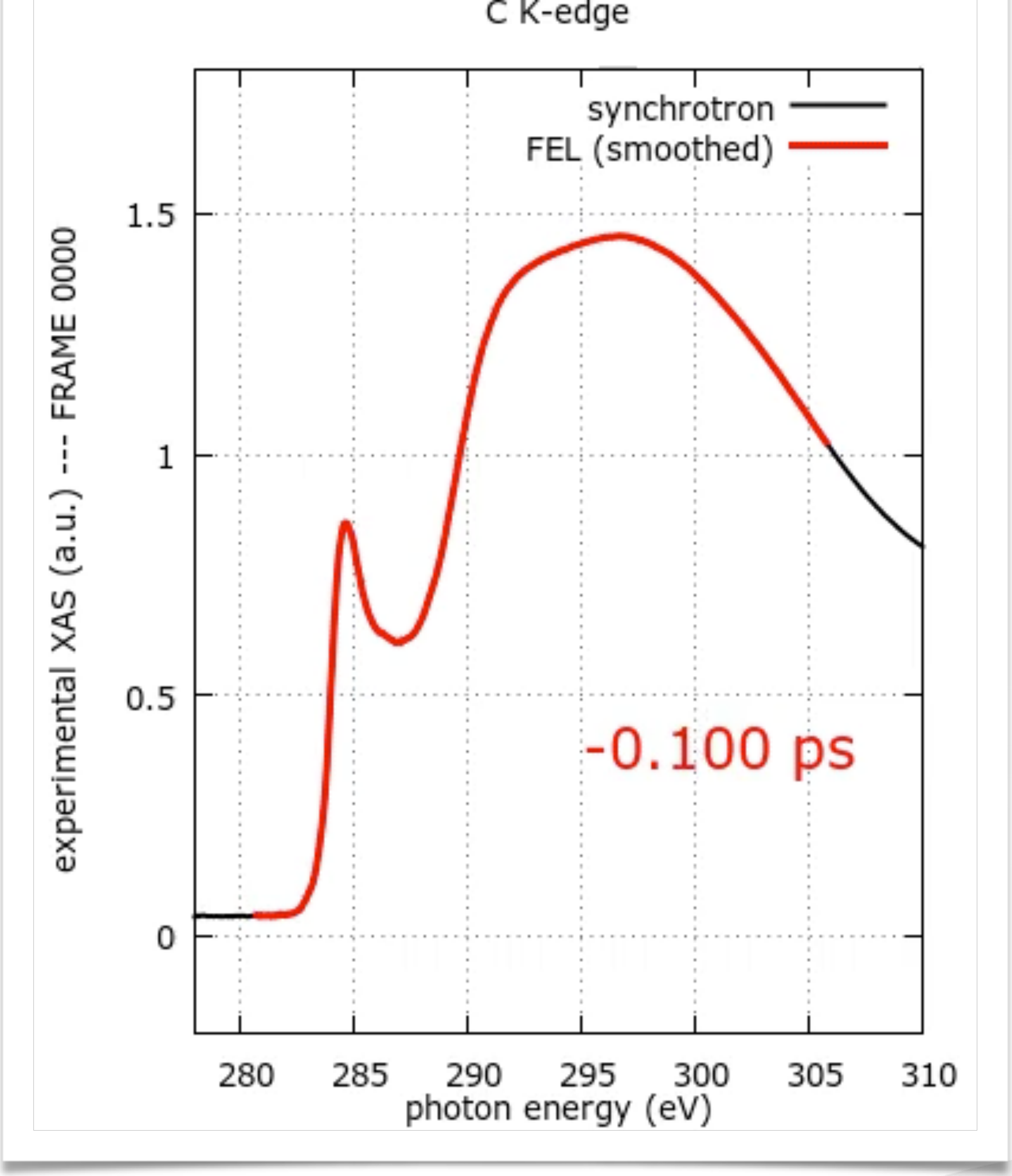

Conclusions

- Elettra and FERMI are producing high level multidisciplinary research
- Openness to the international research community is a key factor for the success of a large scale research infrastructure
- A healthy balance between user research, collaborations, internal research is needed
- Multi method and multi facility studies are becoming more and more common and this must be considered

Conclusions

- Elettra and FERMI are producing high level multidisciplinary research
- Openness to the international research community is a key factor for the success of a large scale research infrastructure
- A healthy balance between user research, collaborations, internal research is needed
- Multi method and multi facility studies are becoming more and more common and this must be considered

Scientific success is a key factor for the credibility with sponsoring institutions, as witnessed by the ~200 M€ Elettra 2 upgrade program

Elettra
Sincrotrone
Trieste

www.elettra.eu